Geoderma 376 (2020) 114541

Contents lists available at ScienceDirect

Geoderma

journal homepage: www.elsevier.com/locate/geoderma

The overlooked soil carbon under large, old trees

Christopher Dean[a,*], Jamie B. Kirkpatrick[a], Richard B. Doyle[b], Jon Osborn[a], Nicholas B. Fitzgerald[a], Stephen H. Roxburgh[c]

[a] School of Technology, Environments and Design, University of Tasmania, Private Bag 78, Hobart, TAS 7001, Australia
[b] Tasmanian Institute of Agriculture, University of Tasmania, Private Bag 98, Hobart, TAS 7001, Australia
[c] CSIRO Land & Water, GPO Box 1700, Canberra, ACT 2601, Australia

ARTICLE INFO

Handling Editor:

Keywords:
Large tree
Primary-forest
Lignomor
Soil organic carbon
Climate-change
Land use change

ABSTRACT

Typical soil organic carbon (SOC) measurements do not account for the higher SOC concentration adjacent to, inside and under the trunks of large trees, or for the root volume which displaces soil and thereby reduces spatial density of SOC. Any net difference between these two omissions could have a significant impact on carbon accounts for the conversion of a primary forest with large trees to a type of land cover with much smaller trees, or no trees, such as to a secondary forest on short harvest cycles, or to deforested land, respectively. To improve knowledge of carbon stocks in primary forests, for better carbon management and climate change modelling, we sampled SOC and soil bulk density directly under large tree trunks, inside tree trunks, in the humus mounds in the buttress region, and under the humus mounds. The measurements were in primary *Eucalyptus regnans* mixed-forest. SOC was formulated as a function of depth. Adjacent to the trees, 90% of the total cumulative SOC was estimated to be within ~2.6 m of the mineral soil surface. That SOC was compared with an earlier measurement in the same locality of SOC in-between trees, away from the trunk and buttress. The SOC under large tree trunks was about four times more concentrated than in-between trees. Formulae that link SOC, root volume, and buttress shape, to tree diameter and ground slope were applied to forest stands within 54.4 ha of primary forest. When the under-trunk SOC was tallied with the organic soils associated with the buttress region and in nearly decomposed logs, SOC at the unit-area-level increased by ~7% [95% CI: 3–12%] relative to the in-between-tree SOC alone, and the absolute increase was 21 Mg ha^{-1} [95% CI: 10–37 Mg ha^{-1}] of SOC. Our results suggest that, at least for land use change that fells mature trees > 1 m in diameter, there may have been higher greenhouse gas emissions from past forest attrition than have been inferred. Globally, we identified 50 example tree species, other than *E. regnans*, that may also have extra SOC at the stand-level in the absence of fire. Additional SOC per hectare was positively correlated with basal area of trees, which increases with the number of large trees in a stand. The maintenance of large trees will help ensure higher levels of forest carbon. The protection of medium-sized trees will be necessary to ensure existence of large trees in the future.

1. Introduction

Land use change (LUC) has caused anthropogenic greenhouse gas (GHG) emissions over millennia (Caseldine and Hatton, 1993; Dixon et al., 1994; Edney et al., 1990; He et al., 2014; Houghton et al., 2012; Luo et al., 2015; Metz, 2009; Olofsson and Hickler, 2008; Pinter et al., 2011; Rhemtulla et al., 2009; Rudiman, 2003; Salinger, 2007). In this work we use the acronym LUC for land use change for forest, such as to arable land, or conversion of primary forest to logged forest, introduction of livestock, increase in fire frequency, or change in logging intensity. A quarter to half of anthropogenic emissions remain in the atmosphere for 500–10,000 years (Archer et al., 2009; Eby et al., 2009; Houghton et al., 1994). Between 40 and 60% of all anthropogenic greenhouse gas emissions from the late Pleistocene period to the present day (from LUC, fossil fuels and concrete manufacture), have remained in the atmosphere (House et al., 2002; Rafelski et al., 2009). Emissions from some major past land use changes are ongoing because of the millennial equilibration time of some soil carbon pools (Dean et al., 2017; Dean et al., 2012b; Hibbard et al., 2003; Khomo et al., 2017). Better knowledge of carbon emissions from LUC is needed (Scharlemann et al., 2014) to improve climate change modelling and for planning climate change mitigation. Improving our knowledge of carbon flux associated with forest conversion requires, *inter alia*, determination of the influence of mature trees on soil organic carbon

* Corresponding author.
E-mail address: christopher.dean@utas.edu.au (C. Dean).

https://doi.org/10.1016/j.geoderma.2020.114541
Received 6 February 2020; Received in revised form 11 June 2020; Accepted 12 June 2020

(SOC), prior to conversion.

Spatial heterogeneity in SOC, which arises from geological, topographic and biogenic features, has been insufficiently represented when measuring change in SOC (ΔSOC) (Conant et al., 2003; García-Oliva et al., 2006). There is likely to be a change in soil organic carbon in the long term, associated with the process of conversion of primary forest to production forest, pasture or herbaceous crops, though controversy currently surrounds its measurement (Dean et al., 2017; Guo and Gifford, 2002; Murty et al., 2002). One of the greatest impediments to measuring ΔSOC due to LUC involving forests is in achieving spatially equivalent sampling before and after logging or fire.

Prior to logging or broad-acre clearing, soil sampling by augering or pit digging near and under large trees and large logs is usually difficult due to the physical obstacle of the wood (Dean et al., 2018). The larger the tree, the further from its centre the obstacles extend. We apply the term 'large' to forest trees that have surpassed silvicultural maturity and are approximately at the peak size of mature individuals for their species and environment, usually with a diameter, at 1.3 m from the ground (DBH), over a metre wide (Dean et al., 2018, Supporting Table S1).

Many obstacles to soil sampling where large trees had grown are removed by clearfelling and related landscape clearing. Soil previously close to the trunk is often mixed with that between trees. If the concentration of SOC is higher closer to large trees, comparisons of SOC before and after disturbance are likely to be invalid.

There is likely to be a concentration of SOC under, in, and around tree trunks, sourced from stemflow, root exudates, decomposing roots and stems, and litterfall. This increase in carbon density is usually belowground in the mineral soil, but for some species there is also SOC in thick humus layers around their trunks (Dubeux et al., 2014; Liski, 1995; Lutz, 1960; Rossetti et al., 2015; Throop and Archer, 2008). In a converse effect, the coarse roots of large trees displace soil (including stones) upwards and outwards (Hoffman and Anderson, 2014; Richter et al., 2007; Šamonil et al., 2018), thereby reducing SOC per unit area, in the vicinity of the trunk. The net effect of these two factors for live trees is unknown. Accounting for the volume of decomposed wood under stumps a century or two after logging can increase the SOC per unit area by ~9% (Sucre and Fox, 2008; Sucre and Fox, 2009), though the authors did not calculate the countervailing coarse root volume of the live trees.

There is a need to refine our knowledge of the soil carbon in primary forests by collecting data on SOC and roots close to and under the trunks of large, mature trees. These data will contribute to improved LUC calculations, fully-coupled climate change models, and dynamic global vegetation models (e.g. Ostle et al., 2009). To the best of our knowledge the SOC under the trunks of large trees in primary forests has not been measured.

Primary forests dominated by *Eucalyptus regnans* in Tasmania, Australia have amongst the highest aboveground carbon concentration per unit area of any forest (Fedrigo et al., 2014; Hickey et al., 2000; Keith et al., 2009; Wood et al., 2010), especially so for the mixed-forest form of *E. regnans* (Fedrigo et al., 2014), the largest patches of which survive in southern Tasmania. For example, primary *Sequoia sempervirens* (Coast Redwood), *E. regnans* , and *Agathis australis* forests have been recorded with carbon in aboveground biomass of 2332, 697, and 435 Mg ha^{-1} respectively (Fedrigo et al., 2014; Sillett et al., 2019; Silvester and Orchard, 1999). For several decades *Eucalyptus regnans* in Tasmania were the most sought after timber species in Australia, as a major contributor to the international paper supply sourced from the Pacific region (Dean et al., 2012c). However, any ΔSOC associated with logging of the species, which started in the late 19th century in Tasmania for lumber, has not been included in national GHG accounts. The high carbon content of *E. regnans* forests, when mature, makes them likely candidates for detection of any influence on SOC concentration linked to individual-trees, by allowing a higher signal-to-noise ratio than for smaller or juvenile trees with a high stand density. Another reason why these trees may produce a high signal-to-noise ratio is that they have several factors known to concentrate rainfall into a high stemflow. They have canopy gaps (being 'open forests' with ~8–20 trees/ha at maturity), tall height (75–110 m), ~45° branch angle and a smooth upper stem, all of which affect the individual tree micro-environment to the extent that rainforest species are hemi-epiphytic on their buttress (Dean et al., 2018; Galbraith, 1937; Hickey et al., 2000; Levia and Frost, 2003). Large *E. regnans* trees could be expected to contribute considerable SOC by central root sloughing during maturation (Ashton, 1975; Braakhekke et al., 2013). The aboveground buttress ecosystem might also leak carbon to below the humus mounds. These regions of the SOC pool are very likely to be affected by LUC.

The aim of the present work was to increase the accuracy of SOC stock measurement, which in turn should aid in determining the fate of forest soil carbon under LUC. The experimental section of the paper has two main parts. Firstly, we studied the soil associated with large trees, across a wide area of forested landscape. Specifically, we sought to quantify previously disregarded parts of the forest soil carbon pool associated with proximity to large trees: the SOC in the buttress region, both above and below ground, underneath, inside and near tree trunks; and the SOC in decomposing logs distributed more broadly throughout the forest. These measurements were used to parameterise formulae to represent the soil carbon in terms of tree size and coarse woody debris size. A measurement of the soil carbon in between such trees in the same study locality was obtained from an independent study. Secondly, we measured the size and amount of carbon in trees (live and dead) and in coarse woody debris (CWD), in a single primary forest stand that was within the broader study area. By applying our formulae derived in the first section to these size data for an exemplar primary forest, and using the independent in-between tree soil measurement, we were able to calculate how much soil carbon is typically overlooked.

2. Methods

2.1. Study site

The study site was 'mixed-forest', which is a type of rainforest consisting of an upper, tall, open-canopy forest of eucalypts above a closed-canopy understorey of callidendrous-rainforest species (Gilbert, 1959; Kirkpatrick and DellaSala, 2011). It was in the Styx Valley, Tasmania, Australia (Fig. 1). The eucalypt canopy was mostly *Eucalytpus regnans* (swamp gum/mountain ash) with small numbers of *E. delegatensis/E. gigantea* (gum-top stringy bark/alpine ash) and *E. obliqua* (stringy-bark/messmate). The rainforest understorey species were predominantly *Nothofagus cunninghamii/Lophozonia cunninghamii* (myrtle/myrtle-beech), *Atherosperma moschatum* (sassafras) and *Phyllocladus aspleniifolius* (celery-top pine). The oldest mature *E. regnans* in the study site were about 520 years old with some signs of senescence (Wood et al., 2010). The effect of fire on the major carbon pools, species distribution and age structure is described in the Supporting Information.

The fire severity and frequency in the study region relate to carbon stock by determining the tree species and size, the depth and longevity of the humus layer, and the size and longevity of logs on the ground (Ashton, 1981; Cremer, 1962; Gilbert, 1959). The eucalypt stands can be killed by severe wildfire, after which an even-aged stand of *E. regnans* grows. The rainforest understorey is uneven-aged but its oldest members can be as old as the eucalypts. Some of the forest stands in the region were uneven-aged, due to less-severe wildfires (Turner et al., 2009). In moist gullies and depressions, where fire is far less-frequent (e.g. once every 1000 years), there are no eucalypts. If severe fire is too frequent then mixed-forest is replaced by wet-sclerophyll forest (Kirkpatrick et al., 1988), which is likely to be less carbon rich.

At Maydena, ~6 km to the north: annual rainfall from 1997-to-2017 averaged 1133 mm, mean daily minimum temperature of the coldest month averaged 2.2 °C, and the mean daily maximum of the warmest month averaged 22.4 °C (Commonwealth of Australia, 2018). However,

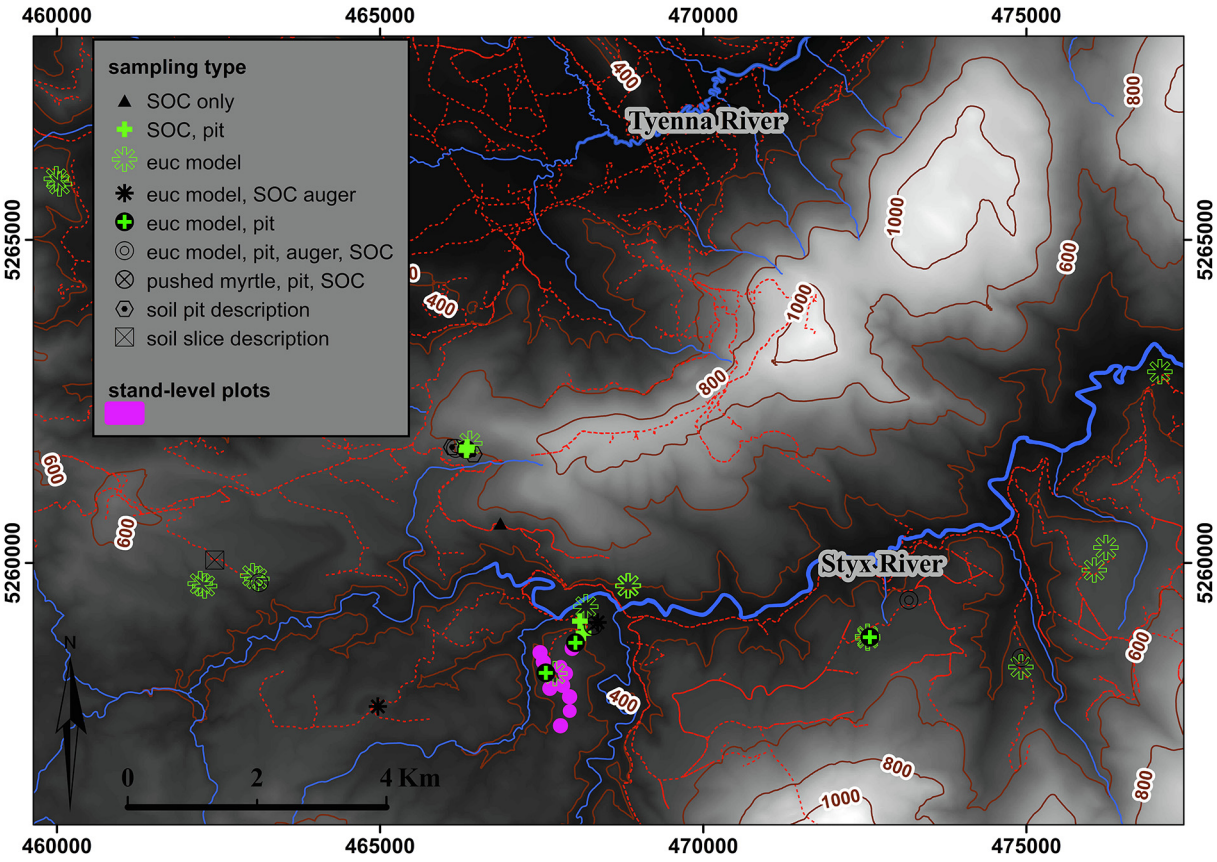

Fig. 1. Study area showing sample types in Styx Valley and Tyena Valley. 'euc model' = 3D model of *in-situ* eucalypt buttress (from Dean et al., 2018), 'SOC' = soil organic carbon sampling for carbon assay and bulk density, blue lines = rivers and named creeks, red lines = roads. Datum GDA 1994, projection MGA, zone 55, metres. For location of this region in Australia see Dean & Horn (2018). (For interpretation of the references to colour in this figure legend, the reader is referred to the web version of this article.)

the average temperature was ~1.4C cooler 60 years ago and rainfall has dropped by ~6% over the last 40 years (Supporting Information).

The soils in the area are derived from sedimentary rocks, mostly finer sediments of the Parmeener supergroup. They are mountain forest soils, being mostly moderately to strongly leached (podzolic) (Wilde, 1946) to pseudogleyed (Schaetzl and Thompson, 2005). The typical profile of the mineral soil in between trees is an A horizon of silty clay-loam from 0-to-0.15 or 0.5 m, a B horizon of gritty, silty light clay from 0.15 or 0.5-to-0.6 or 0.9 m, and followed by a C horizon of light clay, shale fragments and mudstone. Major exceptions are discussed below (section 3.1). The geology of the subset of the main study site, used for the stand-level measurements only, is Permo-Carboniferous sediments, except for the most southerly plot which had Cambrian metamorphic sandstone and mudstone (MRT, 2011).

2.2. Terminology

Soil organic carbon density is the mass of SOC per unit volume of soil, in kg m^{-3}. The unit-area SOC stock is the amount of SOC per unit area (Mg ha^{-1}) in the soil: it is the vertically projected, two-dimensional SOC density. One Mg is one metric tonne. The 'footprint' of a tree is the area inside a convex hull polygon (the minimum enveloping polygon) that circumscribes where the outside of buttress spurs (the protuberances from the lower stem that extend to form large lateral roots) merge with the forest floor (Fig. 2.b, Fig. 3) (Dean et al., 2018, Fig. 2). The forest floor is the layer of material including the litter, fermentation and humus layers above the mineral soil's A horizon. The humus mounds at the base of large trees are called 'duff mounds' in the USA; Ryan and Frandsen (1991). The humus first fills the gaps between the buttress spurs, then, where it decomposes slowly it may cover the spurs. CWD, which includes large branches or fallen tree trunks, lies on top of, or within, the humus mounds, and more generally across the forest floor or streams, in between trees. The humus mounds also contain roots. 'Lignomor' is decomposed, structure-less wood (Green et al., 1993) and is a type of soil, sometimes called 'soil wood' (Jurgensen et al., 1997).

The soil sampling zone underneath the trunk will be called 'u-t' and the zone under the humus in the buttress region will be called 'u-h' (Fig. 2.b, 4.c, 4.d). The u-t zone was surrounded by the u-h zone (Fig. 2b). The 'u-t' zone was directly under the cross-section of the trunk at 1.3 m aboveground (where the DBH measurement was taken). It was approximated as circular in projection, with of diameter = DBH and area = $\pi(DBH/2)^2$. The error in assigning this diameter could possibly be as high as 30%, as judged from digging inside hollow trees and below fallen trees, but it errs on the side of underestimation as the u-t soil was higher in carbon than the u-h soil and was often observed to go beyond the DBH diameter for larger trees.

2.3. Soil sampling and analysis

The most theoretically sound method to determine total SOC for a locality is to measure the whole soil profile as a single unit. This can be done either by analysing all the soil dug from a pit, or by extracting a representative number of entire profile cores then measuring their carbon content. These methods were impractical for our site because neither the necessary machinery nor samples could be transported over the remote, rugged, mountainous terrain without the use of destructive vehicles or pack animals. Although the stand-level measurements of trees were taken in primary forest, the soils were sampled across a larger area that included both primary and recently logged forest. In the

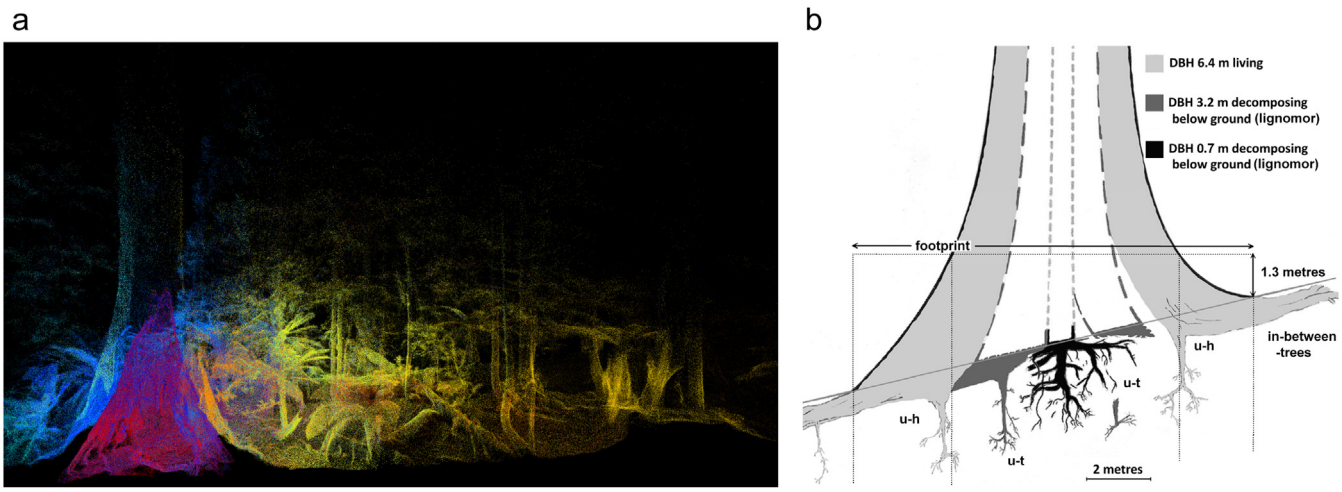

Fig. 2. (a) Example cross-section of mixed-forest. Base of 'Cave Tree' on left, a *Eucalytpus regnans* tree in the Styx Valley, DBH = 5.15 m, with a 'walk-in' hollow (red cone); surrounding understorey; and CWD in centre. Data collected with Zebedee, a mobile, terrestrial LiDAR, data processed by Robert Zlot and Michael Bosse of CSIRO, rendered by current authors using Meshlab. (b) Growth stages of a single *E. regnans* tree, in cross-section, showing fate of decomposed central roots, and zones of SOC measurement below the solum surface: u-t (under-trunk), u-h (under-humus), and in-between-trees. The in-between-trees zone shown here is within 1.5x footprint, so unlikely to have been measured in typical, earlier SOC measurement. Aboveground shape drawn from taper formulae adjusted for ground slope (Dean and Roxburgh, 2006), roots drawn from our observations and literature (Ashton, 1975; Dean et al., 2018). Two hollowing scenarios portrayed, representing encountered variability between trees: (i) left hand side of mature tree hollow (matching Fig. 2a), (ii) right hand side solid. A third scenario observed (not drawn): left hand side hollow but full of lignomor up to 2 m above ground level. (For interpretation of the references to colour in this figure legend, the reader is referred to the web version of this article.)

logged forest, only the rare, minimally disturbed trees were sampled, e.g. felled but only lightly scorched on the outer surface and no manual surface disturbance. Logging allowed soil augering and sometimes pit digging directly underneath the trunks of recently large, healthy, mature eucalypt trees. Two live, large, mature eucalypt trees, the 'Cave Tree' (Fig. 2a) and 'Chapel Tree', had trunk hollows that could be entered through large basal fissures ('walk-in trees') for augering and pit digging (Fig. 4c, d).

Several pits were dug beside or underneath trees that had been measured and detailed by photogrammetry, in order to determine the general nature of the soil horizons. In the pits the soil pH for the surface (0–0.05 m) and subsurface soils (0.05–0.55 m) were determined with a field testing kit (Raupach and Tucker, 1959), accurate to 0.5 pH units.

Soil samples were collected from inside trees, under trunks, and just outside of the trees in and below the humus in the buttress region near the buttress spurs, that is, all soil samples near the trees were sampled within the tree footprint. Hollow trees, without a hole connecting the hollow to the outside world, contained soil in the form of lignomor, above the outside ground level. That lignomor was sampled. In general the depth of soil sampling was from 1.6 m below the old mineral soil surface to 2 m above it (Figs. 3–5). The numbers of samples taken from the different types of locations are shown in Table 1: a total of 92 soil samples were subjected to elemental analysis and bulk density determination, from 17 different tree bases. The forest floor in-between-trees, was not measured in the present study but was measured by (Dietrich, 2012) and was included in our stand-level comparison calculation. This component forms about 1.8% of the total forest C down to 0.3 m, for the forest type studied (Fedrigo et al., 2014).

Soil samples were collected primarily with hand auger equipment: an Eijkelkamp© soil corer (Eijkelkamp Agrisearch Equipment, Giesbeek, The Netherlands) with the sample contained in a sampling ring of 0.05 m height within the bulk density head. Both bulk density and carbon density were determined from the same sample. The augering procedure followed that described in Roxburgh et al. (2006). Augering was performed both in pits and directly from the surface. A total of 15 pits were dug. The number of samples at each location was determined in part by practicalities. For example, the trunk hollows in some trees were narrow—allowing sampling of only one profile, whereas others were wide—allowing a pit and multiple profiles (Fig. 4). The depth of the u-t lignomor was measured by probing with the auger connecting rods.

Soil samples were air dried at 20 °C. A higher temperature was not used, to minimise loss of volatile carbon before the elemental analysis was performed (Thomas and Martin, 2012). Stones > 0.01 m and roots > 0.0005 m in diameter were removed from the samples, weighed, and their volumes measured by water displacement and by a micrometre, respectively. Samples destined for elemental analysis were ground in a mortar and pestle followed by grinding to a fine powder using a ball mill (MM200 Mixer Mill, Retsch GmbH, Haan, Germany).

Removed stones were ground separately and assayed for C, as if they were soil. Bulk density of the soil samples, and hence carbon density of the soil, were adjusted for root volume by assuming that the roots contained no soil carbon. Stone organic C was re-included as SOC because significant amounts of organic C can be dissolved into stones or adsorbed on their surface, with significant contribution to total SOC (Harrison et al., 2003; Zabowski et al., 2011).

The pH of 38 representative distinct soil samples was determined after drying and grinding, by two-point calibration of a Hannah pH Meter on a gently stirred mixture of 1:5 soil:distilled water.

Total nitrogen, carbon and hydrogen elemental analysis in 93 soil samples was performed using a Thermo Finnigan EA 1112 Series Flash Elemental Analyser.

Pedogenic carbonates may precipitate as an illuvial horizon as high up as at −3(0.4) m from the solum surface under 1130 mm year^{-1} rainfall (Royer, 1999) (the rainfall of our study site). Effective rainfall was lower under tree trunks, which could mean that the depth at which carbonates precipitate was within the sampling depth of the present work. This necessitated checking SOC for inorganic C, as opposed to assuming it was all in organic form. The amount of inorganic carbon was checked in six representative soil samples to determine if it was necessary to measure it for all soil samples. The analysis method is described in Supporting Information and the result is mentioned here as it was used to determined part of the SOC analysis protocol. The highest inorganic C proportion, was for one stone at a depth of 0.785 m below the solum surface at 5.8% of total SOC: the average proportion of inorganic C was only 2% of total C (SD = 2%, range = 0.27–5.8%).

Fig. 3. Example soil core locations. 3D-model from Dean et al. (2018). Cross-section and top view of *E. regnans* stump after logging, DBH = 3.11 m (same tree as in Fig. 4.f, 4.g), showing upper parts of augered core locations: two cores in the under-humus region and one in the under-trunk and inside tree (lignomor extended to aboveground). Lower parts of auger holes not modelled as inaccessible to camera. Humus cores not all shown. Height shown on cross-section refers to tree measurement, whereas soil augering used local height basis. Dark red (inner) line = 1.3 m stem contour, blue (middle) line = DBH tape at 1.3 m, brown (outer) line = tree footprint. (For interpretation of the references to colour in this figure legend, the reader is referred to the web version of this article.)

Stones were infrequent in the cores. Therefore, the portion of soil carbon that was not derived from forest biomass was negligible, and the low pH of the samples did not justify further assaying for inorganic carbon. (Low pH means that inorganic carbonates were likely to be dissolved and leached.)

Data from u-t and u-h were processed separately. SOC density data for all the soil samples that were aboveground and inside-trees were not differentiable and were merged, similarly for data from the humus mound. The humus mounds were littered with CWD and humus mound sampling included sampling under logs. In between trees, one transect pit was through a relatively small piece of CWD (0.4 m wide) and the soil around it, and no substantial difference in the soil profile compared with the more-general profile in-between-trees was observed, compared with the large contrast to the u-t region. That sub-CWD zone was not sampled further. SOC data away from trunks, the large-tree footprint and large roots, i.e. SOC in-between-trees, were from Dietrich (2012) who measured from −0.45 to 0 m from the mineral soil surface. In that research the soil was sampled from dug holes, with removal of three layers of approximate depths 0–0.15, 0.15–0.3 and 0.3–0.45 m of $9.4(\pm 5.6) \times 10^{-4}$ m^3 each, which were individually homogenised. It is unlikely that soils were sampled under CWD.

2.4. SOC data processing

When determining SOC stocks for the soil profile at the unit-area-level there are several ways to take samples, measure C, process the data and tally. Rarely is a comprehensive depth of the soil profile measured even though it is known to be the most accurate method to get SOC per unit area (Ngo et al., 2013). Instead, usually either a formula is fitted to the data down to a limited depth (e.g. 0.3 m) then extrapolated downwards, or those data are erroneously implied to represent the entire SOC stock. The latter approach can create misconceptions when measuring change in SOC (ΔSOC) with LUC. Another method of calculating ΔSOC is to measure a constant mass of mineral soil (Gifford and Roderick, 2003), but that method is applicable where the soil profile and nature of the change are well defined and the amount of change is known to be minor compared with the original SOC stock.

For estimating cumulative SOC per unit-area as a function of depth, we employed three established methods and one new method. The three established methods were less suitable to the soil profiles of our study site than that used (Supporting Information). When deriving formulae, parameters were refined by nonlinear regression using LABFit (da Silva and da Silva, 2015) as described in Dean et al. (2018).

We introduce a new method that allows the use of SOC measurements taken over a broad range of depths rather than requiring measurements taken from predetermined soil horizons. The method is suitable for merging data with spatially and vertically diverse SOC densities. Data were collected at a wide range of depths because of the irregular nature of the sampling environment, *viz.* large, cut stumps with lignomor in the trunk hollow above the level of the outside mineral soil surface; cavernous, live hollow trees; fallen trees; and deep humus between buttress spurs (Fig. 4). For integration to get cumulative SOC down the profile, depth was divided into 0.001 m intervals. Thus, the SOC density data from any one 0.05 m high sampling ring, gave 50 equal data points (Fig. 6). Data points from different locations but for the same 0.001 m depth interval, were averaged. Any depth intervals with no measurement were assigned the average value from the nearest measurements above and below it. The interval data were then tallied to give cumulative SOC with depth, from the solum surface down to the deepest measurement. Interval data not corresponding to the centre of any sampling ring position were not used in further processing, i.e. the number of data points used in further processing equalled the number of original soil samples. The process was carried out separately for u-t and u-h. The cumulative SOC data were formulated as a simple exponential function of depth:

$$cumulative\_SOC = g[1 - \exp(bz)] \quad (1)$$

where *cumulative_SOC* is in $Mg{\cdot}ha^{-1}$, and gives the cumulative unit-area SOC with depth, and *z* is the distance from the solum surface (in metres, negative below 0 m). Eq1 was differentiated to yield SOC density:

$$SOC\_density = gb[\exp(bz)]/10 \quad (2)$$

where *SOC_density* is in $kg{\cdot}m^{-3}$, and b, g and z are as in Eq1

Inside the centre of tree trunks, the lignomor was continuous across z = 0 m height [at the level of the mineral soil surface outside the trunk]. Thus, data above and below 0 m but within 0.025 m (half the sampling ring height) provided a reliable value for SOC density at 0 m (termed 'C0′), and this value was used in the method entitled 'fixed C0′.

Equations were fitted to three main regions: u-t, u-h, and in between trees, the latter based on the raw data from Dietrich (2012) (Table 2). Equations for u-t SOC were trialled with and without the value at z = 0 m being held constant at C0.

2.5. Stand-level effects

2.5.1. Tree measurement

The stand-level geometric measurements were taken in a sub-set of

Fig. 4. Examples of soil sampling environments and methods used for four example *E. regnans* trees. Tree 1: felled during logging, DBH = 4.38 m, (a) augering under-trunk, (b) sliced humus mound and bared roots. Tree 2: live, 'Chapel Tree' DBH = 6.08 m, (c) digging pit under-trunk, (d) 0.94 m of red lignomor under-trunk, above mineral soil, (e) profile in humus mound, and pit under-humus. Tree 3: felled during logging, DBH = 3.11 m, humus profile, and pit and augering under-humus, same tree in Fig. 3: (f) left side of Fig. 3, (g) right side of Fig. 3. Tree 4: burnt during logging later fell, pit under-trunk, using bulk density head, (h) red lignomor, (i) mineral soil. Distance between red marks on scale bars = 1.2 m. (For interpretation of the references to colour in this figure legend, the reader is referred to the web version of this article.)

the larger area used for soil sampling. They were collected from 10 circular plots of outer radius 60 m, totalling 11.2 ha, between November 2010 and April 2015. The plots were randomly located (using a random number generator and accommodating plot size) across 54.4 ha of remnant primary mixed-forest, in scheduled logging coupe SX009B (Fig. 1). The furthest distance between circular plots was 1.3 km, and they had a range of topographies and forest types, including uneven-aged, even-aged mature, and mature-senescent.

The main tree measurement taken was DBH. The angle of the girth measurement was adjusted from the horizontal for stem slope. For larger trees, which all had vertical stems, the horizontality of the girth tape was checked with a clinometer. Ground slope was also measured as were the main dimensions of CWD. Measurement methodology, including DBH, and CWD dimensions and decay category (soft, medium or hard) followed the protocols in Dean et al. (2012a). Fieldwork volunteers were trained by scientists and deployed to measure the DBHs and CWD (i.e. 'citizen science'). For quality control in data processing, any data outliers that appeared possibly spurious (e.g. very large or very small), were rechecked mathematically, and, if necessary, the data point was re-measured.

Measurement error in DBH was estimated to be 5%, and in each dimension of CWD it was estimated to be 10%. These values were obtained by comparing numerous measurements and some re-measurements. Error margins were intentionally increased two-fold after data processing to acknowledge that larger errors occur when measuring larger trees (Butt et al., 2013).

Existing allometric equations based on DBH and ground slope (Dean et al., 2018) were used to calculate buttress, humus mound and root, volumetric characteristics. The allometric equations enabled scaling-up to give SOC at the stand-level. The root volume of snags (standing dead

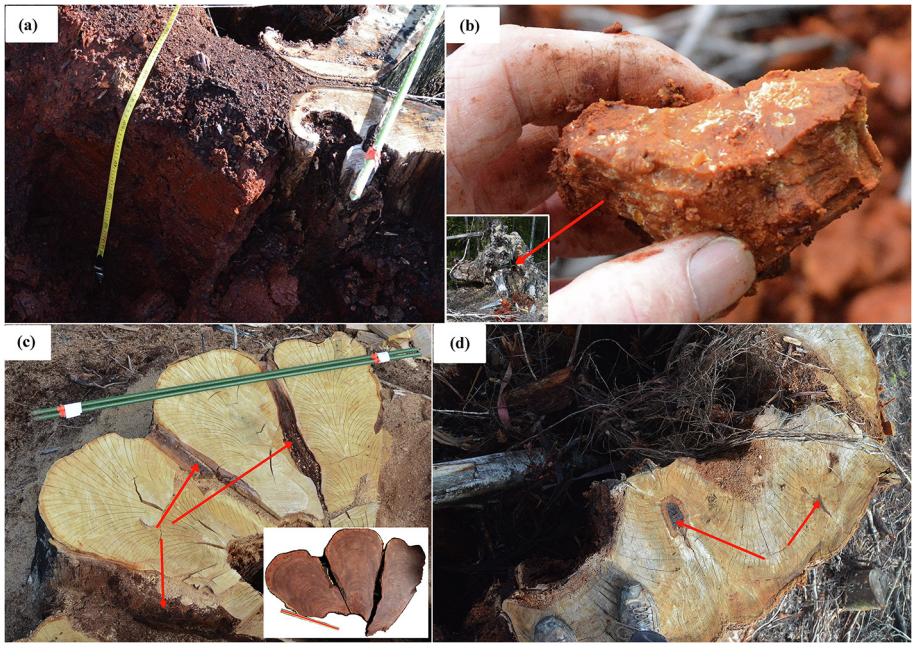

Fig. 5. Example lignomor pools not included stand-level tally. (a) Aboveground red, friable, wet lignomor at least up to 1.4 m inside hollow *E. regnans*. (b) Aboveground lignomor from hollow myrtle tree: cunncaseus (Dean and Horn, 2019) with tell-tale conchoidal fracture and yellow colour (inset: parent myrtle pushed-over during logging). (c) Bark on flutes at 1.3 m becomes trapped as spurs grow then bark decomposes into lignomor (arrows) (inset: sanded cross-section, growth rings showed early spur development), (d) continued spur growth joins spurs together, isolating lignomor, and trunk cross-section becomes more circular. (For interpretation of the references to colour in this figure legend, the reader is referred to the web version of this article.)

trees) at the stand-level was calculated using the formula for live *E. regnans* (Dean et al., 2018, equation (11)). The snags were assigned a fractional presence based on the CWD decay classification (hard = 1, medium = $^{2}/_{3}$, soft = $^{1}/_{3}$). The volume of soil displaced by large roots for each tree (Dean et al., 2018, equation (11)) in the stand-level data was tallied to adjust the SOC per unit-area. Using the same allometric equations, a spatial simulation of typical soil sampling in a forest stand, which uses predetermined locations and the common practice of moving sampling points away from large trees, was performed as a diagrammatic aid to show sampling effects.

The allometric equations used to determine C in individual live *E. regnans* trees (Dean et al., 2012a; Dean et al., 2003; Dean et al., 2004) included adjustments for locally observed senescence, maximum tree size and age (i.e. potential growth for the site). Although primary forest, the study area was a vestige left from the State-wide, industrial process that had sourced timber from the most carbon-dense forests over several decades, i.e. high-grading (Dean et al., 2012c). Therefore, the study area was not one of the more-C-dense sites possible in the region. The allometric equations had been developed from a larger range of tree sizes than the trees measured in the present study, but from trees with the same degree of senescence and similar fire histories. This meant that extrapolation was not necessary. For example, the maximum DBH observed for trees used in the earlier 3D-modelling (Dean et al., 2018) was 7.16 m but the largest tree in the present study had a DBH of 5.20 m.

For application of the allometrics to determine tree C content, the parameter 'mid-year of senescence' was set at 550 years and the parameter 'rate of senescence' was set at –10 (Dean et al., 2003 Table 3.1, Eq.8). The productivity multiplier (related to the forest science 'site index') for DBH was set at 1.880 (Fig. 7). The parameters were selected to match the ~500 year old, large, mature *E. regnans* in the region (Mount, 1964; Wood et al., 2010) with the maximum DBH of trees in the plots. These parameter settings simulated the biomass peaking at 400 years (i.e. peaking prior to senescence) and gave a DBH of 5.3 m at 500 years. To get the simulated DBH to more closely match the observed 5.20 m would have required a second iteration of simulation but it was not considered necessary. With these parameter settings the aboveground C for *E. regnans* trees peaked when DBH = 4.94 m, attaining 62.4 Mg (after which the biomass decreased with increasing DBH), which compared well with that of 58.7 Mg from formulas in Sillett et al. (2015) (which did not model senescence). This forecast amount of carbon versus DBH, for the local *E. regnans*, was then cast as a single formula by modelling, using Eureqa:

$$Eregnans\_C = 3.394142 DBH^{2}\{1/[1 + \exp(5.081129 DBH - 27.68206)]\} \quad (3)$$

where *Eregnans_C* is in Mg and *DBH* is in m. This formula was applied to the stand-level DBH data, to tally the amount of carbon from *E. regnans* at the stand-level. For total understorey biomass, the multiplier for

Table 1
Average attributes for specific soil types. Only from cores without contaminates of other soil types. Standard deviation in brackets, except for when N ≤ 2 where it is the measurement error.

Soil type		Num. obs. (N)	Distance from solum surface (m) (Error ± 0.02 m)		Bulk density (kg m^{-3})	C density (kg m^{-3})	C wt%	C/N	H_2O wt%	pH
			min	max						
Lignomor without cunnite		29	−1.07	2	238(59)	115(29)	48(3)	128(70)	70(11)	2.9(0.3)
Lignomor with cunnite		30	−1.07	2	274(201)	138(129)	48(3)	128(69)	68(15)	3.0(0.3)
Non-lignomor mineral soil		37	−1.6	-0.115	1090(403)	31(25)	6(11)	24(12)	27(15)	4.0(0.5)
Mudstone in deepest cores		2	−0.611	−0.785	3380(225)	16(16)	0.47(0.43)	17(11)	48(8)	3.95(± 0.02)
Inside-tree	Aboveground	9	0	2	270(82)	131(43)	48(2)	187(88)	66(18)	3.2(0.7)
	Belowground (u-t)	51	−1.6	−0.025	749(718)	70(44)	25(22)	64(50)	50(24)	3.6(0.6)
Outside-tree	Aboveground	8	0.05	1.36	279(125)	91(13)	37(11)	34(7)	57(14)	3.4(0.2)
	Belowground (u-h)	19	−1.40	−0.05	1070(403)	32(20)	7(15)	22(7)	24(8)	3.8(0.3)

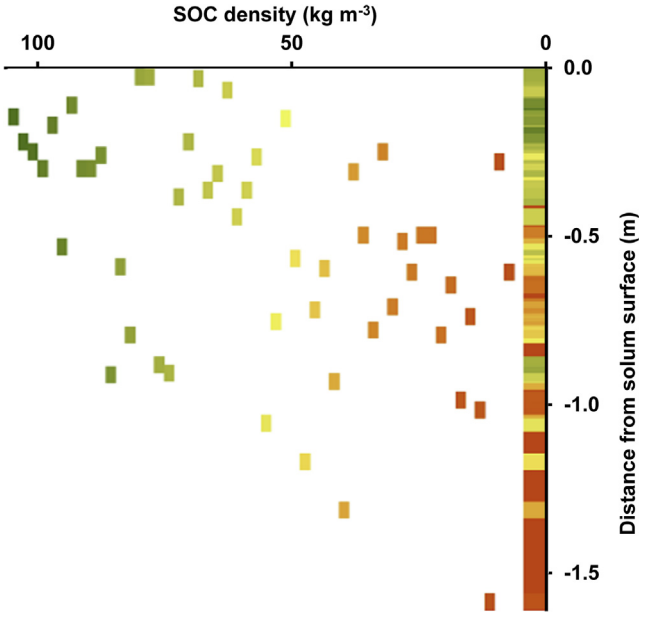

Fig. 6. Schematic illustration of our new method, using inside-tree data. Concentration data are position-coded and colour-coded: green and left = high-SOC grading linearly to brown and right = low-SOC. Each coloured box represents a sampling point with a sampling-ring, with the ring height of 0.05 m having 50 × 0.001 m intervals. The coloured column is a 1D representation for visualisation purposes only. (For interpretation of the references to colour in this figure legend, the reader is referred to the web version of this article.)

understorey biomass in the understorey allometric equations was 0.5 (Dean et al., 2012a; Dean et al., 2004).

2.5.2. Tallying below-ground SOC

The u-t and u-h areas of soil were tallied for all live trees and snags > 0.2 m DBH. Trees with DBH < 1 m were assumed to only have half as much u-t SOC as those with DBH ≥ 1 m because the smaller trees had not developed buttresses and would be mechanically unstable if most root volume under the trunk had decomposed to form lignomor. The under-trunk SOC from snags was assumed to be present on a pro-rata basis according to their decomposition category (1, $^{2}/_{3}$ and $^{1}/_{3}$ for hard, medium and soft respectively). For example, a 'soft' category of dead tree was two thirds of the way to being entirely absent from accounts. That is, it was assumed that the degree of decomposition in the roots of snags was the same as for their aboveground components.

2.5.3. Tallying SOC in and under the humus mounds

The equation for humus volume as a function of a tree's footprint (Dean et al., 2018, Equation 9) was applied to each live eucalypt tree with DBH ≥ 1 m. The humus volumes were then summed at the stand-level. This was converted to SOC ha^{-1} using the SOC density for the humus mound of 91(SD = 13) kg m^{-3} (Table 1). The total SOC beneath the buttress humus mounds was determined by combining the equation for humus area (Dean et al., 2018, Equation 8) with the cumulative under-humus SOC (u-h). Understorey trees, were not noted to have humus mounds. Many understorey trees were hemi-epiphytes on the eucalypts and therefore any humus arising from them may well have been already counted. Snags were modelled as having no humus mounds. A few eucalypt snags had vestigial humus mounds but generally the humus volume was minimal, as litterfall decreased with advanced senescence, and epiphytic trees gradually died with the decrease in host-tree stemflow.

Minor carbon pools not included in the stand-level tally are listed in Supporting Information and shown in Fig. 5.

2.5.4. SOC in well-decomposed logs, 'soft-logs'

It was necessary to consider at what stage CWD becomes soil and therefore should be tallied with other SOC. A three-category classification system was used in the present work for CWD (hard, medium and soft). From a comparison of our CWD decomposition stages with those in the literature (provided in Supporting Information) it seemed conservative to infer that half of the mass in the soft log category was SOC rather than wood. It is likely that there is also SOC in 'medium' class CWD but the proportion is too indeterminate to include here and in order to remain conservative with respect to SOC, it was excluded.

At the stand-level, half of the soft-log C was added to the SOC tally. The soft-log volume was converted to mass using a conservative basic density of 400 kg m^{-3}, and multiplied by the decay class (0.3333), then half of that dry mass was assumed to be soft-log C (Dean et al., 2012a).

2.5.5. Comparing the effects of between-tree SOC with all stand-level SOC

The data of Dietrich (2012) for mixed-forest were used as the background benchmark to which the effects studied in the present work were compared mathematically. The study of SOC in-between trees by Dietrich (2012) included five mixed-forest plots in the Styx, Tyenna and Florentine valleys. His broader study area included ours and one of his plots was centred within our stand-level site. His work included 31 samples from mixed-forest. The forest-types in that study were similar to those in the present work: primary mixed-forest, mostly *E. regnans*-dominated but Dietrich (2012) had higher amounts of other dominant species: 20% *E. delegatensis*-dominated, 20% *E. obliqua*-dominated, and 20% myrtle-dominated.

The SOC was firstly calculated for the 10 plots in the present work using the Dietrich (2012) data for in-between trees. The SOC was then calculated by replacing the areas 'under-trunk' and 'under-humus' with the SOC values calculated in the present work, then adding the humus mound SOC. To quantify any difference in total SOC for forest stands (compared with the in-between-tree SOC), results were expressed as a percentage difference: the 'Extra-SOC', relative to SOC stocks based on sampling the in-between-tree areas only, giving:

$$\text{Extra-SOC} = \sum \text{Extra-SOC}_i = \sum 100 \times (New_i - Old)/Old \quad (4)$$

where $Extra\text{-}SOC_i$ is the percentage change summed over each stand-level feature type, i, tallied in the present work, *Old* is the default stand-level solum SOC derived from Dietrich (2012), and New_i is the SOC for feature type i. Features include u-t SOC, u-h SOC, humus SOC and soft-log SOC, and the first three were each separated into three groups of trees: live 0.2 m < DBH < 1 m, live DBH ≥ 1 m, and snags (except no humus for snags, as described above). As an example of how $Extra\text{-}SOC_i$, was calculated, consider i = u-t for live trees with DBH ≥ 1 m:

$$\text{Extra-SOC}_i = 100 \times \frac{((b \times u) - ((1 - b) \times Old)) - Old}{Old} \quad (5)$$

where b is the basal area for live trees with DBH ≥ 1 m in ha ha^{-1} (not m^2 ha^{-1}), u is u-t SOC for those trees in Mg ha^{-1} and $Extra\text{-}SOC_i$ is percentage change. For the lignomor in soft-logs the projected area of

Table 2
Solutions to Eq1. Standard deviation in brackets. Regions: 'u-h'= outside tree, within footprint, below-ground; 'u-t'= inside tree, below-ground.

Region	g (Mg ha^{-1})	P(t)	b (m^{-1})	P(t)	adjR^2	Df	P
u-h	516.312 (23.688)	< 0.0005	0.840134 (0.058057)	< 0.0005	0.997	18	$< 5 \times 10^{-8}$
u-t	1202.23 (33.69)	< 0.0005	0.992529 (0.041934)	< 0.0005	0.995	56	$< 5 \times 10^{-8}$

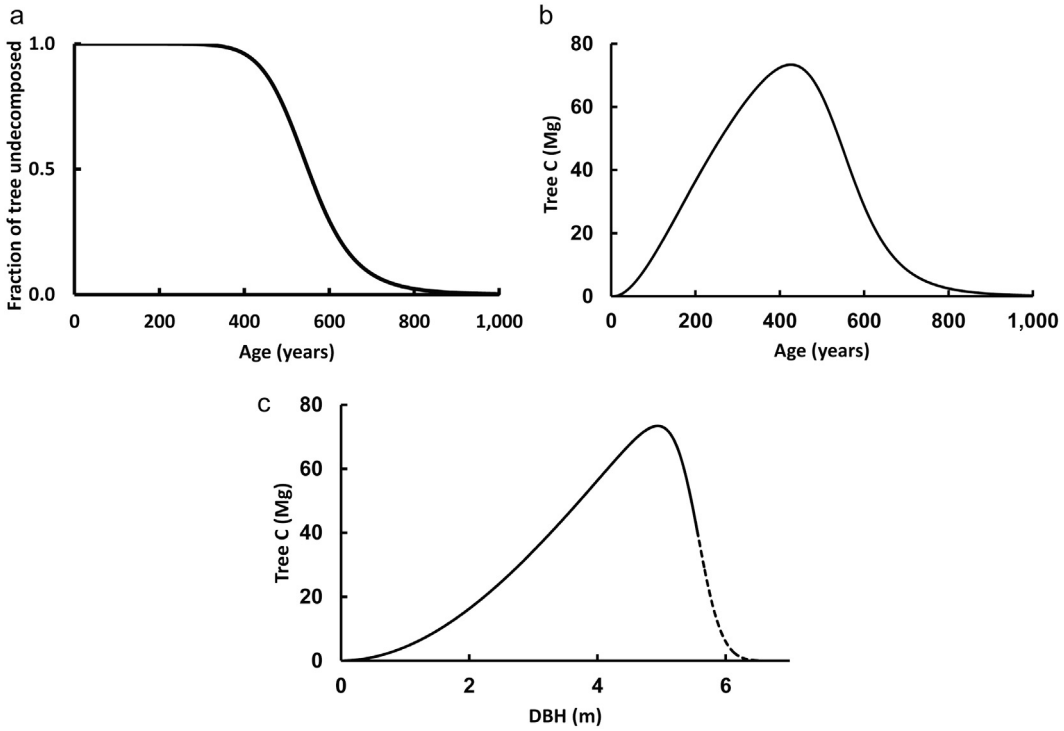

Fig. 7. Adaptation of *E. regnans* formulae in Dean et al. (2003) and Dean and Roxburgh (2006) for SX009B. (a) Fraction of tree that is undecomposed, as a function of age (i.e. inverse of fraction senesced), (b) whole tree carbon versus age, derived by multiplying '(a)' by un-senesced tree carbon vs. age, and (c) whole tree carbon versus DBH, derived from '(b)' by inverting the equation for age as a function of DBH, note high DBH tail is dashed to indicate some trees of this advanced age may have lost girth at 1.3 m. Note that these adaptations were designed for a somewhat depauperate mixed-forest stand (compared with those logged earlier) in coupe SX0009B in the Styx Valley, and different parameter settings would be needed for sites of very different productivity or fire regimes.

the individual logs was used and '*Old*' was the carbon in the forest floor (not the solum). A sensitivity analysis was performed by calculating the effect on *Extra-SOC* from varying *Old*.

3. Results

3.1. General soil characteristics

The soils were either podzolic or pseudogleyed mountain forest soils, apart from three main exceptions. Firstly, soil under the trunks of large trees was dominated by an irregularly shaped bowl of lignomor ~1 m deep but deeper where coarse roots had penetrated further down (measured up to 2.3 m deep by probing with the auger connecting rods). Beneath the lignomor the clay was not affected by either leaching or waterlogging, unless rain had leaked into the top of the tree hollow, in which case there was a weakly bleached horizon under the lignomor. Such bleaching was thicker when more water had entered. Where rain was able to enter the main trunk hollows, some roots and more mineral soil areas were observed within the lignomor body. Secondly, if the surface water outside of the trunk in the buttress zone could not flow due to impediment from the tree's roots and bedrock, then there was a redoximorphic environment, with gleying and the smell of H_2S. Thirdly, in some locations there were buried albic A horizons, at up to 1.4 m from the solum surface, including their *in situ* charcoal from a forest fire when that horizon was at the top of the soil. These layers had been penetrated and disrupted by tree roots. Localised deviations from the usual soil type described above for the study site were found near the buttress, for example:

(a) on the downhill side of a large *E. regnans* (DBH = 4.38 m): Sapric Histosol, and
(b) on the uphill side of a medium-sized *E. regnans* (DBH = 3.11 m), where the bedrock was high and relatively impervious and the ground was steeply sloping, trapping topographic flow: Histic Stagnosol.

From roadside cuttings it was observed that there were large undulations in the depth to the bedrock surface (e.g. from 0.1 to 1.7 m depth, within 3 m horizontally), with matching undulations in mineral soil depth, but without noticeable corresponding variation in the biomass of *E. regnans*. The bedrock was highly fractured and did not appear to impede root penetration.

The pH values for lignomor (except cunnite, a dense dry lignomor in myrtle beech trees, Dean and Horn (2019)), and non-lignomor soil in the vicinity of lignomor, were 'ultra-acidic' (terminology of Rayment and Lyons, 2011), whereas all other substances were only 'extremely acidic'. The value for non-lignomor solum under the trunk, of 3.40 (SD = 0.24), was similar to the value of 3.6 (SD = 0.6) for Tasmanian rainforest soil (di Folco and Kirkpatrick, 2013). The lignomor was more acidic, with pH = 2.73 (SD = 0.12). Stones in the vicinity of lignomor had pH = 3.95 (Table 1). The bulk density of lignomor was linearly negatively correlated to $\%H_2O$, with $R^2 = 0.65$, $P < 1 \times 10^{-7}$.

3.2. Soil carbon density and cumulative SOC

Bulk density vs. soil carbon (C) wt% showed a hyperbolic relationship (Fig. 8), as noted elsewhere (e.g. Hiederer and Köchy, 2011; Huntington et al., 1989; Périeé and Ouimet, 2008). This relationship held across a wide range of C densities, from stones to lignomor, up to C 50 wt%:

$$bulk\_density = a + b\sqrt{Cwt\%} - c\ln(Cwt\%) \quad (6)$$

where *bulk_density* is in kg m^{-3} and *Cwt%* is the percentage carbon of soil by weight, a = 1408.2(64.6) kg m^{-3}, P(t) < 0.005, b = 72.959(46.135) kg m^{-3}, P(t) = 0.117; c = 431.41(70.67) kg m^{-3}, P(t) < 0.005; df = 88, adjR^2 = 0.78, (probability) $P < 0.005$. A

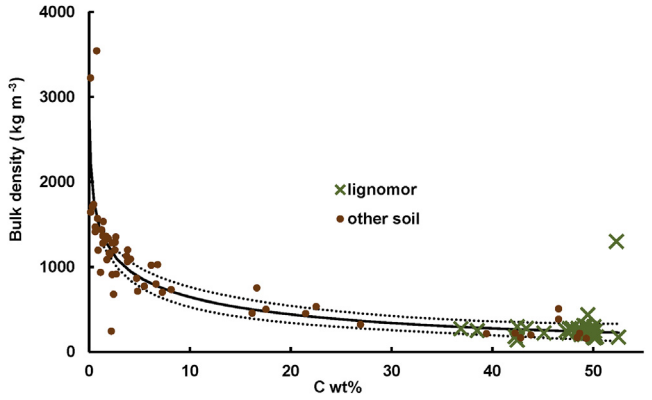

Fig. 8. Bulk density vs C wt%. Solid, black curved line represents Eq 6. Dotted lines are 95% CIs. The outlier at the right-top is cunnite, which was not included in the regression.

range of other equations with similar fits are given in Supporting Information. On visual appearance, the next best option for our data after Eq 4, was an equation of the form: $bulk\_density = a + b\sqrt{\text{Cwt\%}} - c\sqrt{\sqrt{\text{Cwt\%}}}$ (parameters in Supporting Information).

Relatively high variability in under-trunk C density (Fig. 9.a) arose from the contrast between lignomor and the mineral soil, and the spatial variability of areas that previously had been roots. The effect of fixing SOC density at 0 m to the lignomor average (C0) was negligible because it only had a localised effect (Table 3).

The eucalypt under-trunk lignomor and inside-hollow lignomor were burnt to varying extents after fire (Fig. 10). This carbon pool was diminished by varying degrees even after one fire in the Styx Valley even when the trees survived the fire. It was depleted to a greater extent after intense logging burns. In the drier forests across Australia where fire is more frequent, such as the Jarrah forest in Western Australia, under-trunk lignomor was not observed where fire had entered basal trunk hollows.

The SOC that could be practically measured in routine future experiments was considered as being represented by 90% of the cumulative [calculated] total SOC. Within the tree footprint, 90% of the SOC was calculated to be within ~2.6 m of the old mineral soil surface. For the in-between-tree cumulative SOC data derived from Dietrich (2012), 90% was within ~1.6 m (Table 3). There was substantially more cumulative SOC (Table 3, Fig. 9.b) closer to trees than in-between-trees:

Table 3
Cumulative SOC, and depth at 90% of total. Numbers in brackets are 95.4% confidence intervals. Regions: 'u-h' = outside tree, within footprint, below-ground; 'u-t' = inside tree, below-ground.

Restraint	Cumulative SOC (Mg ha^{-1})	Depth at 90% of total (m)
	u-t	
C0 at 0 m	1202 [1137, 1277]	−2.32
none	1223 [1152, 1306]	−2.44
	u-h	
none	516 [473, 572]	−2.73
	in-between-trees, derived from Dietrich (2012)	
none	309 [295, 324]	−1.59

4x for under-trunk and 1.7x for under-humus.

The 95% confidence intervals appear narrow because of the mathematical dependency of the error margins of processed SOC values on merged data (for shallower levels) and fine-scale interpolated points (in the new method we developed). Therefore some of the variability of the deeper data is obscured.

3.3. Stand-level carbon

In our 10 plots the overall effect of including near-tree SOC in mixed-forests, the 'Extra-SOC', was 7% [CI: 3–12%] (confidence intervals are at the 95.4% level henceforth) more SOC than is usually reported for such forests (Table 4). The single largest contributor, at 40%, to the Extra-SOC at the stand-level was from the under-trunk region of living trees, this being from decomposed roots (Fig. 4c, d, Fig. 5a, Fig. 11). The majority (67%) of that came from eucalypts, and of that, 66% from eucalypts with DBH ≥ 1 m. The under-trunk SOC for living trees and snags together contributed the majority (55%) of the Extra-SOC. Also at the stand-level, the under-trunk SOC created Extra-SOC of 2.8% [CI: 1.6–4.0%] (above that if the under-trunk region was occupied by the same SOC density as the in-between-tree value) (Fig. 11), 74% of which was for trees with DBH ≥ 1 m.

At the stand-level, the attributes most strongly correlated to Extra-SOC were the basal area of trees with DBH ≥ 1 m (R^2 = 0.53, P < 0.02), humus volume (R^2 = 0.58, P < 0.02), and the projected area of logs with diameter ≥ 1 m (R^2 = 0.77, P < 0.001).

For eucalypts with DBH ≥ 1 m the SOC stock in the humus mound was only 3.5(SD = 1.1) Mg ha^{-1}, and it raised the SOC per unit-area by 1% [CI: 0.70–1.2%]. The under-humus SOC of eucalypts with

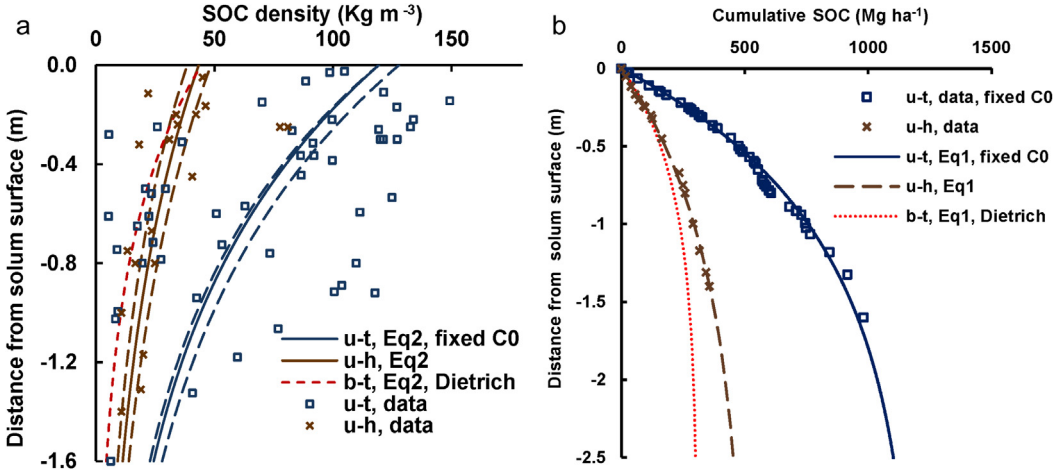

Fig. 9. (a) SOC density location comparisons. 'u-t' = under- trunk, 'u-h' = under-humus area, 'b-t' = in-between-trees. Each regression curve (Eq2) for u-t and u-h, is a triplet, with the two outer curves being 1 standard deviation of regression parameters. (b) Cumulative SOC, data and regression curves (Eq. (1)) for different regions with respect to tree location: u-t = under-trunk, u-h = under-humus-area, b-t = in-between-trees.

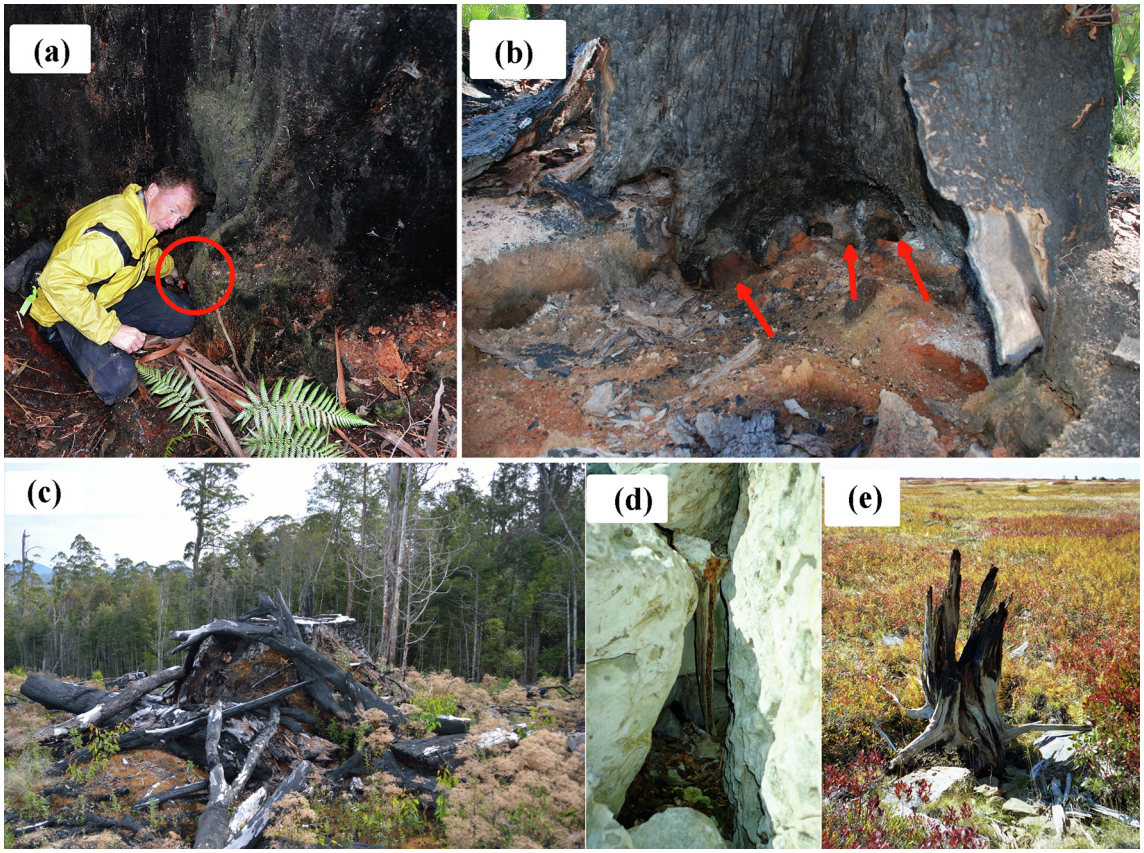

Fig. 10. Regions of loss of lignomor or humus C through LUC. (a) Under-humus root lignomor lost to at least 1.5 m deep (red circle) in a live *E. regnans* due to logging burn (photo: Y. Bar-Ness, 2013). (b) Under-trunk and under-humus lignomor lost in a live *E. marginata* (jarrah) Western Australia due to prescribed burning. (c) Logging debris piled on *E. regnans* buttress to ensure humus, rainforest epiphytes are burnt during logging. (d) and (e) Roots bared after forest floor humus layer burnt during logging about a century ago, Dolly Sods, West Virginia, USA. (For interpretation of the references to colour in this figure legend, the reader is referred to the web version of this article.)

Table 4
Stand-level effect of 'extra-SOC' on cumulative SOC (to 90% of total), compared with in-between-trees (Dietrich, 2012). Numbers in brackets are 95.4% confidence intervals.

In-between-trees, derived from Dietrich (2012) (Mg ha^{-1})	New total SOC (Mg ha^{-1})	Extra-SOC (%)
All 10 plots		
309	330	6.9 [3.2, 12]
Seven *E. regnans*-dominated plots		
309	332	7.6 [3.6, 13]
Two most C-dense plots		
309	341	10.6[5.0, 18]

DBH ≥ 1 m raised the SOC per unit-area by 0.35% [CI: 0.20–0.60%].

There was 1,273(SD = 45) m^3 ha^{-1} of live-tree coarse root volume close to trunks, with 87% of that coming from trees with DBH ≥ 1 m; and 46(SD = 34) m^3 ha^{-1} from snags. This coarse root volume from live trees and snags reduced SOC stocks by only ~0.63%.

Soft-log C contributed ~34% of the total Extra-SOC (Fig. 11). It must be appreciated, however, that soft-log C is normally counted as CWD C and is therefore already part of typical whole-of-forest estimates. The amount of soft-log volume at the stand-level was 129(SD = 128) m^3 ha^{-1}, half of which was attributed to lignomor: 64(SD = 64) m^3 ha^{-1}, which is less than the volume of decay-class-V CWD found for the same forest type by Dietrich (2012), namely 82 m^3 ha^{-1}. This comparison suggests that the amount of soft-log C was not overestimated in the present work.

The effects of snag under-trunk SOC was approximately the same as

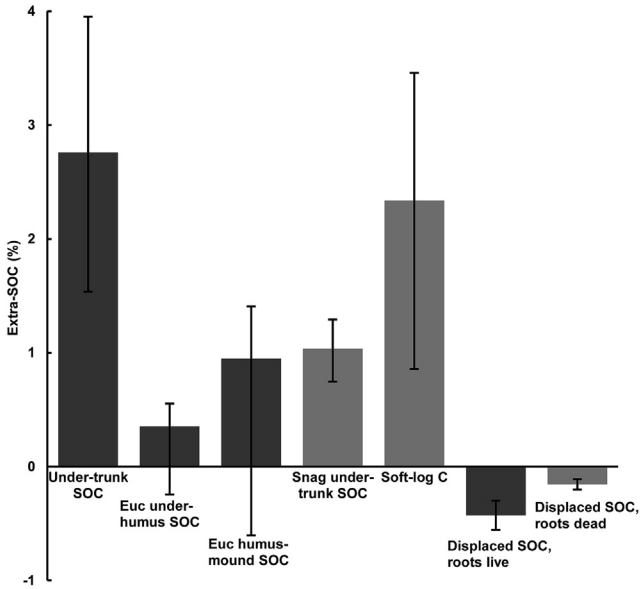

Fig. 11. Overall effect of including near-tree and soft-log SOC on unit-area 90% of SOC stocks. Dark-grey = living trees, light-grey = dead trees.

that of the buttress humus (Fig. 11), 15% and 14% contributions to the Extra-SOC respectively. The smallest single contribution, 5% of the Extra-SOC, is under-humus SOC. The SOC displaced by roots (live and dead) contributes −0.58% to the Extra-SOC.

A sensitivity analysis showed that if the value for in-between-tree SOC (derived from Dietrich, 2012) was changed by ± 20% from 309 [CI: 295–324] Mg ha^{-1}, then the Extra-SOC changed from 7% [CI: 3–12%] to 5.1% or 9.8% respectively. For a very different value for in-between-tree SOC, for example if it changed by ± 50% from 309 Mg ha^{-1}, then Extra-SOC was 3.9% or 16%, respectively, which is close to our CIs for Extra-SOC. Therefore, for our estimate of Extra-SOC to be outside the 95.4% confidence limits we obtained, then the value of in-between-tree SOC would need to be ~50% different to the value we derived from the work of Dietrich (2012).

Results in Table 4 are presented for different groupings of the plots: all 10 plots, *E. regnans*-dominated plots only, and the two most-carbon-dense *E. regnans* plots. Sites from the work of (Dietrich, 2012) could not be differentiated into forests types as their SOC values were all within one standard error of each other and the means of the *E. regnans* and *E. delegatensis* forest types were equal to within three significant figures.

For the *E. regnans*-dominated stands only, and especially for the two more-even-aged of those, the change in Extra-SOC from 7% [CI: 3–12%] to 11% [CI: 5–18%] was contributed mostly by large, dead trees. The Extra-SOC for these stands should perhaps be compared with the in-between-tree SOC from that specific forest type rather than with the general in-between-tree SOC of Dietrich (2012) but the standard deviations in that study did not allow differentiation of forest types. A more comprehensive set of observations might show that for different mixed-forest types the percentage Extra-SOC might stay the same although the absolute Extra-SOC (in Mg ha^{-1}) changes.

Regardless, the contribution from snags to the increase in under-trunk SOC and the SOC displaced by roots, were both doubled on going to the two more-even-aged *E. regnans*-dominated stands. The contribution from soft-logs increased by ~70% and the under-trunk SOC for live trees with DBH ≥ 1 m increased by ~45%. Thus, overall, the contributions that increase SOC in the absence of fire for *E. regnans* mixed-forest are from the large trees (dead and alive) and from soft-logs.

The two largest contributions to Extra-SOC shown in the stand-level data were SOC under-trunks and soft-log volume. The Extra-SOC under-trunks with DBH ≥ 1 m was positively correlated with obstructive root volume of living trees: $adjR^2 = 0.97$, $P < 2 \times 10^{-7}$; and this relationship was dependent mostly on the obstructive root volume of eucalypts with DBH ≥ 1 m: $R^2 = 0.85$, $P < 2 \times 10^{-4}$. Therefore, as the root volume from large eucalypts increases and displaces SOC so too does the lignomor from dead roots, which adds to SOC. The second largest contribution to Extra-SOC, soft-log volume, was not significantly correlated with root volume.

The numbers of different tree species measured in the 10 plots was: *E. regnans* 104, *E. obliqua* 7, *E. delegatensis* 25, myrtle 265, sassafras 839, celery-top pine 19, and five other understorey species 10. In terms of the estimated major contribution to biomass in the different plots, seven were *E. regnans*-dominated, one was *E. delegatensis*–dominated, one was marginally *E. obliqua* dominated, and one was rainforest-species dominated. All had substantial amounts of *E. regnans*.

Basal area [of trees] in the 10 plots was 118(SD = 62) m^2 ha^{-1}, of which 52% comprised eucalypts with DBH ≥ 1 m. Eucalypt trees with DBH ≥ 1 m contributed 98(SD = 9)% of the total basal area of eucalypt trees. Carbon in live biomass (including roots) was 462(SD = 137) Mg ha^{-1}, 32(SD = 17)% of which, i.e. 149(SD = 54) Mg ha^{-1}, was from understorey trees. Carbon in logs was 64(SD = 50) Mg ha^{-1}, and C in snags was 62(SD = 61) Mg ha^{-1}. Carbon in live biomass was correlated with the basal area of trees with DBH ≥ 1 m (Fig. 12.a):

$$C\_in\_live\_biomass = (alarge\_BA) + b \quad (6)$$

where *C_inlive_biomass* is in Mg ha^{-1} and *large_BA* is in m^2 ha^{-1}, $a = 5.11034$ Mg m^{-2}, SD = 0.63117, P(t) < 0.005; $b = 117.474$ Mg ha^{-1}, SD = 45.827, P(t) = 0.03; df = 8, $P < 1 \times 10^{-6}$, $R^2 = 0.89$, $adjR^2 = 0.88$, $P < 5 \times 10^{-5}$. The intercept on the ordinate axis, i.e. parameter *b*, represents the average C in live biomass for trees with DBH < 1 m. Trees with DBH ≥ 1 m comprised 69(38)% of total C in live biomass. Eq6 can be used in other mixed-forests on similar sites and with similar fire history, to approximate stand-level biomass, by only measuring trees with DBH ≥ 1 m.

At the stand-level, humus-area was a linear function of basal area of eucalypts with DBH ≥ 1 m (Fig. 12.b):

$$humus\_area = (aeuc\_large\_BA) + b \quad (7)$$

where *humus_area* is in m^2 ha^{-1} and *euc_large_BA* is in m^2 ha^{-1}, $a = 0.713576$, SD = 0.052271, P(t) < 0.005; $b = 8.66461$, SD = 3.480955, P(t) = 0.04; df = 8, $P < 1 \times 10^{-6}$, $adjR^2 = 0.95$.

Stand-level humus-volume was a linear function of basal area of eucalypts with DBH ≥ 1 m (Fig. 12.b):

$$humus\_volume = (aeuc\_large\_BA) + b \quad (8)$$

where *humus_volume* is in m^3 ha^{-1} and *euc_large_BA* is in m^2 ha^{-1}, $a = 0.343093$, SD = 0.086612, P(t) = 0.004; $b = 16.7382$, SD = 5.780, P(t) = 0.2; df = 8, $P < 0.005$, $adjR^2 = 0.62$.

Note that the above equations for humus-area and humus-volume cannot be used directly to calculate humus amounts. However, their parameters when calculated by standardised major axis linear regression in program SMATR (Warton et al., 2006) can be used thus:

in Eq. (7), humus area: $a = 0.7284$, 95%CIs 0.6718–0.8589; $b = 7.728$, 95%CIs: −0.241–15.698

in Eq. (8), humus volume: $a = 0.4126$, 95%CIs: 0.2668–0.662; $b = 11.89$, 95%CIs: −1.39–37.924.

4. Discussion

4.1. Implications and applicability

A previously unmeasured section of the SOC pool was quantified. At the stand-level, large trees provide an extra 5% in unit-area SOC (66% of 6.9%) than previously measured in addition to the SOC in between them. When the under-trunk SOC was combined with organic soils associated with the buttress region and the lignomor in nearly decomposed logs, SOC at the unit-area-level increased by ~7% [CI: 3–12%] relative to the in-between-tree SOC alone. The diagrammatic spatial simulation of typical soil sampling (Fig. 13), shows that it is likely to miss the Extra-SOC in primary forests. The lack of good spatial sampling in the past in primary forests, is therefore likely to have artificially lowered the calculated LUC emission for such forests, if the calculations were based on empirical data, because the places where carbon is concentrated are more likely to be missed before logging than afterwards.

In situations where the upper solum, lignomor and humus mound were mixed during LUC then a consistent omission of 7% prior to LUC would obscure measurable SOC change for several decades. Such LUC could be logging or broad-acre deforestation. That low precision, could contribute to poorer policies for climate change mitigation. The percentage extra-SOC might be higher in other types of forest, if the spatial variation within forest stands is higher.

The biomass of the understorey is commonly less than that of the eucalypts in mixed-forest (e.g. 30(13)% in Dean et al. (2012a) and 33(17)% in the present work) so their decomposed roots should be a minor contributor to Extra-SOC compared with that from dead eucalypt roots, unless they die more frequently than eucalypts or their dead roots have a longer half-life.

The findings here are relevant to the management of the tropics and boreal zones where the largest tracts of primary forests remain (Wirth et al., 2009). They also are relevant to temperate forests such as the Douglas Fir (*Pseudotsuga menziesii*)-dominated rainforests and Coastal Redwoods (*Sequoia sempervirens*) of N. America, which can accumulate humus mounds in the absence of fire (Dominik DellaSalla and Steve Sillett, personal communication, 2015). Many coniferous forests lack high humus mounds around the base of dominant trees, except possibly

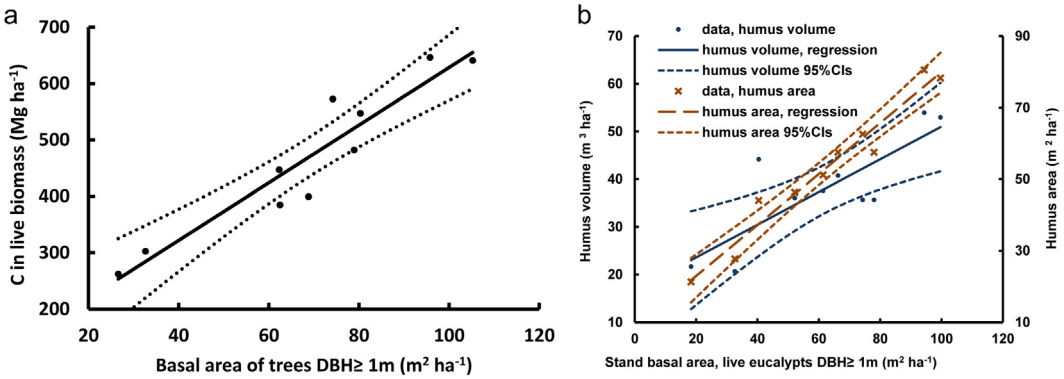

Fig. 12. The stand-level basal area of eucalypts with DBH ≥ 1 m was: (a) the strongest indicator of C in live biomass. (b) the dependent variable in linear relationships to humus-area and humus-volume. (Dotted lines are the 95.4% confidence intervals.)

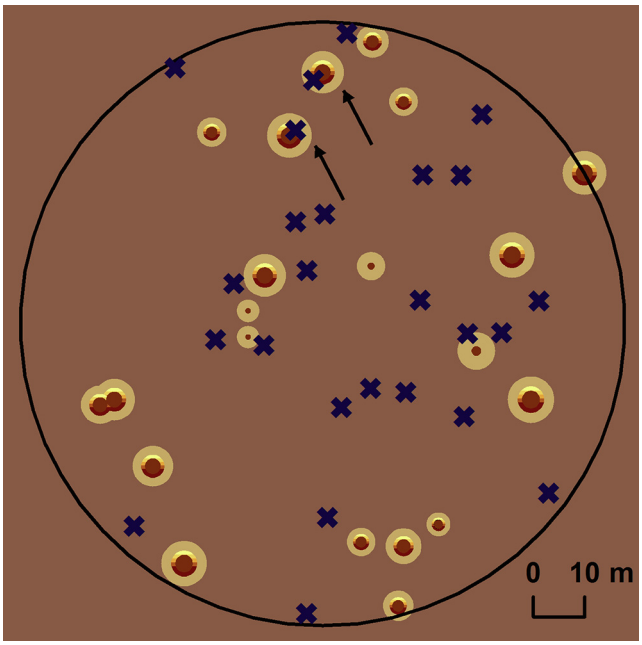

Fig. 13. Schematic of how heterogeneity in SOC is usually missed at the stand-level prior to logging. Spatial distribution of trees with DBH ≥ 1 m in forest plot #8. Circles drawn to scale. SOC levels: central circles = under-trunk, varying shade middle rings = under-humus and humus mound, outer lighter rings = obstructive root zone (1.5x footprint) in-between-trees, background = less obstructed in-between-trees. Crosses = random soil sampling. Where points are selectively excluded (or relocated) prior to logging (for example) due to inaccessibility—pointed to by arrows—sampling would miss more-C-dense areas and obstructive root zones, but less likely to miss them after logging, especially if upper solum is redistributed.

where fire is absent for over a century, but the humus may be more-evenly distributed than in *Eucalyptus* forests. For example, prior to the logging-fires in the Canaan Valley (WV, USA), a climax red spruce (*Picea rubens* Sarg.)-dominated forest in boreal climate conditions, had a widespread, permanent, deep humus-moss layer (Allard and Leonard, 1952) (Fig. 10d, 10e).

Four examples of species of present-day trees that we believe are wide enough and old enough and have not been subject to intense fires, and therefore may have substantial amounts of Extra-SOC under their trunks are: *Quercus robur* (pedunculate oak), *Q. petraea* (sessile oak), *Sequoia semipervirens* (redwood) and *S. giganteum* (giant sequoia). These have formed extensive areas of forests in England and Europe (oaks) and North America (sequoia and redwoods). The oak forests in England were only extensively converted to plantations in the early 20th century whereas those in Europe were removed a couple of centuries earlier. In both cases the effectively millennial half-life of the SOC pool (Dean et al., 2017) means there should still be substantial areas of legacy SOC, a residual from the previous coarse oak roots. The larger oaks have DBH > 2.9 m. In 2017 there were approximately 3300 trees with DBH from 1.9 to 3.3 m (Farjon, 2017). Those 1.9 m wide are ~400 years old, at which age the central roots would have become lignomor. This is only a few trees compared with the *E. regnans* in Tasmania (560 ha logged by CBS per year from 1999 to 2009 (Dean et al., 2012c), with about 10 mature individuals per hectare (Gilbert, 1959): ~5,500 felled annually), but the likely legacy SOC from past forests should also be considered. Young redwoods of ~130 years on rich soils have DBH ~1.4 m (Sillett et al., 2018), which is similar to *E. regnans*. But the redwood is slower growing and more rot resistant (Sillett et al., 2010) with the larger *Sequoia* individuals having a DBH up to ~7 m (Williams and Sillett, 2007) and longevity around 2000 years. They are likely to have central lignomor beneath their trunks, possibly more than *E. regnans* due to their continued growth and higher basal area per hectare (Sillett et al., 2010). Globally, we identified 50 examples of tree species other than *E. regnans* that may also have Extra-SOC, from lignomor under the trunks of mature individuals, at the stand-level in the absence of fire (Supporting Table S4).

Higher stocks of SOC can also be reported from deeper soil sampling and deeper soils (James et al., 2014; Jobággy and Jackson, 2002). In the present study the organic C density in bedrock (mudstone) was non-negligible: about half that of the non-lignomor mineral soil (Table 1). The mudstone was approximately half water and thus susceptible to organic C addition from DOC. Additionally the upper bedrock was fragmented, thereby possibly distributing C to deeper rocks. The effect of not measuring the entire profile on the calculated SOC per unit area is not known due to the contrasting influences of rocks containing organic C and possible transport of C in groundwater. However, it is most likely to be a minor contribution to the penultimate error margins as it is likely to affect both under-tree and in-between-tree equally. The zone under CWD was not measured in the present work, though it can have higher SOC than in the open forest floor, at least in the top 0–0.1 m in mesic forests (Błońska et al., 2019; Lodge et al., 2016). It appears unlikely that the extra SOC under CWD away from trees would be more than that under the humus mounds, which also have CWD and have additional C from stemflow.

The SOC associated with large trees, such as in the humus mounds, decomposing coarse roots (u-t), decomposing logs, and DOC (Tipping et al., 2012), although most often unmeasured, is inherent (though undifferentiated) in many carbon dynamics models where SOC in the models is derived from tree carbon, but is treated as homogenous in 2D or 3D. Tuning such models requires adjustment of bulked-SOC half-lives to match observed SOC stock, by calibrating model parameters (Hararuk et al., 2014). Therefore their accuracy is a function of the

accuracy of SOC sampling. In turn, such modelling is part of fully-coupled climate change models, which makes them also dependent on the SOC sampling.

4.2. Soft-log SOC

Logs may cover up to 12–20% of the ground area in mature and oldgrowth Douglas Fir-Western Hemlock (*Pseudotsuga–Tsuga*) (Harmon et al., 1986). The integration of well decomposed CWD into the forest floor matrix may be a slow process (Strukelj et al., 2013). The present study suggests that a portion of decomposed logs are already SOC, as lignomor. If some portion of 'decay class-IV' is also empirically determined to be lignomor (less decayed than class-V) then even more C should be re-assigned to the SOC pool. Attributing soft-log C to the soil pool rather than the CWD pool may be controversial, but the re-assignment will help rationalise carbon dynamics modelling, easing hiatuses therein. Many reports on carbon stocks, which are used to calibrate models, have followed IPCC recommendations (IPCC, 2003) of recording all log mass as 'dead wood' (i.e. allocated to the CWD pool): 'Includes all non-living woody biomass not contained in the litter, either standing, lying on the ground, or in the soil.' The models gradually allocate portions of the CWD to the emission and SOC pools as time passes, so the model outputs may be missing SOC or counting some C twice.

Alternatively, for consistency in carbon accounting, if soft-log C is not considered as SOC then neither should decomposing roots, which would need to be reassigned as CWD. Subsequently that volume could not be considered as soil and therefore the soil bulk density and SOC at the stand-level would both need to be decreased. Indeed, some authors refer to a decay class system for coarse roots, although the most decomposed category (possibly lignomor) was most likely too malleable to be measured by the vertical probing technique employed (Mobley et al., 2013). Thus, it was inadvertently considered as soil, though typically it is not measured as soil during soil sampling. In forests elsewhere, SOC can also be on branch forks and adventitious growths (e.g. Sillett and Bailey, 2003; Sillett and Van Pelt, 2007; Wooley et al., 2008). In general, the mineral soil and forest floor are not tight boundaries for soil carbon accounting.

4.3. Relation to literature reviews on LUC

Some meta-analyses have drawn conclusions on the fate of SOC for conversion of forest to pasture or to cropland, and vice-versa. For example in one meta-analysis Guo and Gifford (2002) found an average increase in SOC of 8%, for conversion of native forest to pasture. Some of the data points in that study were for LUC of primary forest, and the higher concentrations of SOC near the trunk centres may not have been measured. Thus, the long-term spatial imprint left in the soil by mature trees (Døckersmith et al., 1999; Phillips and Marion, 2005) may well influence calculations of a representative value for grasslands that used to be forests. Additionally, some of the forests included in that global average were tropical with substantial lateral groundwater flows of deep SOC (Johnson et al., 2008), whereas grasslands have relatively shallow and more easily observed SOC (Canadell et al., 1996). The Guo and Gifford review has been cited ~2500 times, and their 'forest to pasture' finding cited ~320 times (Google Scholar©, as of April 2018), thus, possibly influencing policy and climate change. If that 8% increase was reduced by 7% for the SOC not measured under large tree trunks before LUC then that result would cease to be statistically significant. In turn that could have altered the choice of land use activities over the last decade, possibly making them less damaging to the global climate. Similarly, if the 'no detectable change' upon forest to pasture conversion found by Murty et al. (2002) (cited ~780 times) was reduced by 7% then a decrease in SOC may have become the significant finding. The changes to the reported findings would of course depend on the types of forest prior to LUC, for example: how many had SOC originating from large trees that prevented spatially representative soil sampling.

4.4. Limits to applicability

There are two scenarios in which under-trunk SOC is unlikely to contribute as strongly as it does in Tasmanian *E. regnans* forests. Firstly, fire increases basal fissures (Adkins, 2006) and thereby increases the probability of emission of inside-tree lignomor to the atmosphere. There was depletion in drier forests elsewhere in Australia, which have higher wildfire frequency than *E. regnans* forests. Secondly, in some forests the trees may be older than the half-life of the central under-trunk lignomor, which may thus have long-since decomposed (e.g. *Sequoiadendron giganteum*).

Additionally, if SOC was found to be spatially homogenous and unrelated to tree location, then it would indicate that the findings in the present work were inapplicable. Schöning et al. (2006) could not detected spatial variation in SOC in younger forest with an inter-tree distance of 7 m. However, they postulated that that was due to either the SOC of the previous forest masking the present forest, or to innate differences in the soil. More commonly, surface litter fall and tree roots are found to affect microbiology and SOC with spatial patterning reflecting tree species and location at a scale of centimetres to several metres (Bruckner et al., 1999; Finzi et al., 1998; Prescott and Grayston, 2013; Saetre and Bååth, 2000). The two of our plots with the most mature-only *E. regnans* had 15.63 trees ha^{-1}, which gives an average inter-tree distance of 25.3 m, or 17.9 m for tightest circle packing, filling ~76% of the space. Both spacings allow SOC heterogeneity.

The selected equation for soil bulk density as a function of C wt% contained a natural log term. At values of C approaching 0 the function for bulk density approaches infinity, so one of the other equations listed in Supporting Information may be more suited to, for example, quartz sands. The ln term allowed the curve to match our mid-range and end data values. For a deep profile soil with moderate amounts of SOC and negligible stone content, the reciprocal equation may be better suited as it has a low bulk density when SOC = 0. It was not necessary to form a log–log relationship for bulk density versus C wt% as in, for example, Huntington et al. (1989). The choice of curve depends not only on its statistics but also on whether it looks like the curve suits the spread of the data points. If our mudstone data points were omitted then the reciprocal form might be applicable here, but mudstone was a large component of pedogenesis, it contained SOC, was quite common in the area, and was of the same material as the fragmented bedrock. The sqrt, two term equation is another likely fit for our data, and it does not have an extreme asymptote.

4.5. Depth effects

Deep-set SOC can comprise at least half the total SOC in the profile (Harrison et al., 2011) and therefore it is important to include it in SOC sampling but measuring its change with LUC can be problematic. The present study provided indicative depths to sample 90% of the SOC (~2.6 and ~1.6 m for proximal to trees and in-between trees, respectively). Deep-set SOC generally has a greater average age than that in surface horizons (Paul, 2016), e.g. in the order of a thousand years (Rumpel and Kögel-Knaber, 2010), which implies that it generally changes more slowly (e.g. Wendt and Hauser, 2013). Therefore, if there is insufficient time between before-and-after measurements accompanying LUC to allow the soil representing the new ecosystem to reach its representative dynamic-equilibrium, (e.g. when deforesting, reforesting long-cleared land, or changing the dominant tree species), then measuring deeper layers can create misconceptions regarding the effects of LUC. This is not a limit to the results or methods of the present study but a note of caution when applying them.

For SOC analysis in general, it would be pragmatic to provide some limit on the depth to which SOC is tallied. It is necessary to measure

deeper than the shallow sampling (0.3–1 m) initially recommended for Tier 1 and 2 carbon projects (IPCC, 2003), so as to capture changes in the deeper horizons affected by, for example, tree roots, which average several metres deep in temperate forests (Canadell et al., 1996; Harper and Tibbett, 2013; Harrison et al., 2011; Trumbore, 2009). In our study site ~2.6 m was necessary to include 90% of the SOC in the solum (from Eq1 for under-trunk SOC), which would include SOC in some weathered parent material and some DOC that permeates bedrock. Mobile groundwater, found in several places in the study region, would redistribute C, and confound C modelling. The forests dominated by *E. regnans* in the Victorian Central Highlands (VCH) in the State of Victoria mostly lack a rainforest understorey (except in gullies) but have a much greater depth of soil down to bedrock (5–20 m, Ashton, 1975; Polglase et al., 1994) than for our study site in Tasmania (2–4 m). Therefore it is likely that they have a different SOC vertical profile and a different SOC 90% depth limit.

4.6. Anthropogenic impact on the Extra-SOC

The loss of eucalypt under-trunk lignomor and inside-hollow lignomor with fire, is a carbon emission that must be considered in forest management. When undisturbed these lignomors can increase both the stock and half-life of SOC per unit-area. The under-trunk lignomor will influence the spatial heterogeneity of SOC for one or two successive generations of forest, which explains the observed legacy of SOC heterogeneity (Harmon, 2001; Wilson et al., 2010). That legacy is less in secondary forests (Oyarzún et al., 2011). That loss in legacy SOC could reduce soil variability and in turn threaten ecosystem multifunctionality and sustainability, and in so doing, reduce climate change resilience (Havlicek and Mitchell, 2014; Thompson et al., 2009; Wagg et al., 2014).

A reduction in the biomass and associated SOC of large trees in tall open-forests in Tasmania is forecast under climate change (Bowman et al., 2014; Dean and Wardell-Johnson, 2010). Larger trees are already becoming rarer (with secondary-forest growth aside, Kauppi et al. (2015)), due to increase in areas subject to forestry, anthropogenic fire, agriculture and mining; and in some places due to climate change with its variety of longer summers, and increased water limitation and fire severity (Ferguson, 1948; Galbraith, 1939; Hansen et al., 2013; Herrmann, 2006; Jacob et al., 2013; Laurance et al., 2000; Lindenmayer et al., 2012; MacFie, 1999; Mackey et al., 2015; McIntyre et al., 2015; Rankin, 1947; Slik et al., 2013). In the short-term, large-tree-decline will increase SOC through a sudden increase in lignomor. However, in the long-term, that lignomor will not be replenished once it has decomposed as the *E. regnans* cannot mature and become large under severe climate change, therefore the long-term, temporal-average SOC will decrease.

The reduction in forest carbon in some regions due to climate change is a net emission compared with the non-climate change scenario. It is positive feedback, which will in turn increasingly detract from the carbon stores of some forests (Houghton, 1997; Kashian et al., 2006; Warszawski et al., 2013). Decomposition of both below-ground CWD and SOC has been forecast to increase with climate change (Kirschbaum, 2004; Kolchugina and Vinson, 1995), contributing to the positive feedback (Raich and Schlesinger, 1992). The same influences when impacting on the Extra-SOC (but not re-counting the soft-log C), would give a new emission of 5–5.4% of the previously counted SOC.

The positive correlation of Extra-SOC with basal area of eucalypts with DBH ≥ 1 m means that young stands are poor contributors to SOC stocks. There is little scope for mitigating the carbon emissions associated with logging primary forests, except for longer harvest cycles and increased wood-product recycling (Dean et al., 2012c). However, there is a mathematical scenario where young stands may amass high carbon stocks: if the harvest cycle length is considerably shorter than the time taken for root decomposition. In this hypothetical situation over multiple logging cycles root carbon may accumulate to form a large underground biomass pool and eventually a large SOC pool. However, the mass of undecomposed roots may reduce water infiltration and tree productivity, and hence the theoretical, high carbon sink may not eventuate.

The maintenance of large trees, with their localised high concentrations of SOC, will help ensure higher levels of forest carbon storage. This is significant also because the region has been subject to high-grading (logging of the larger, more densely packed trees, earlier) (Dean et al., 2012c). This has implications for LUC accounting on more productive land globally. The protection also, of medium-sized trees, including, if possible, from both direct-anthropogenic and climate-change effects, will be necessary to ensure the large trees of the future.

With 13,545 ha of *E. regnans* primary mixed-forest remaining in 1976 (ANM, 1979) in the Styx and Florentine Valleys the estimate of a 6.9% underestimation for SOC implies an underestimation of 258 Gg [CI: 130–458 Gg] of SOC in pre-logging carbon (if assuming the in-between-tree value of 278 Mg ha^{-1} derived from Dietrich (2012), being 90% of total SOC). This is a conservative estimate as 4000 ha of mixed-forest had already been converted by 1959 (ANM, 1959). The long-term total emission of SOC if logging cycles continue, and assuming a long-term (millennial) decrease in SOC of ~50% (Dean et al., 2012c), is then 2.0 Tg [CI: 1.0–3.6Tg].

Temperate forests currently occupy ~600 Mha worldwide, with most directly impacted by humans (Heath et al., 1993). For example, the area of tall open-forest in Australia has principally been halved since Europeans first settled in Australia (in ~1750) as those forests were either 'mined' for timber or simply cleared for agriculture (Kirkpatrick, 1986; Kirkpatrick, 1994), plus there was clearing for mineral mining and urbanisation.

The existence of higher SOC in remnant primary forests suggests that there are higher emissions from past forest disturbances than have been inferred. Based on examination of remnant primary forests, one could extrapolate to find the historical forest carbon stocks, taking into account that remnants may represent selection bias (Lindbladh et al., 2013). Such legacy Extra-SOC has either been emitted or is in the process of being emitted from the forests cleared from Neolithic times to ~1000AD (Kaplan et al., 2010), and it will be either contributing to global warming or have been re-sequestered in for example, the oceans or recovering forests—contributing to possible future sink saturation.

4.7. Conclusions and further research

The project improved knowledge of carbon stocks and provided useful formulae for application. However, a comprehensive carbon budget for LUC requires more data, such as for forestry activities (Bradshaw et al., 2013). To measure emissions accompanying LUC it may be necessary to isolate and measure its components separately. For example, for 'clear-fell, burn and sow' logging, which has been popular in Tasmania, the influence of burning on SOC could be isolated by using one of the burns that has spread to neighbouring unlogged forest, as a control. The change then being analysed is the felling-only component. The work presented here facilitates such experimentation.

The information on some of the main pathways of ΔSOC is numerically indeterminate and some of the processes are not well understood. For example, how much carbon descends to what depth in highly-fractured bedrock, how far is it carried horizontally by groundwater, and what are the emissions en-route?

One of the lignomor pools that was not counted in the stand-level tally, that in hollow trunks of large trees, is one of the pathways for trunk heartwood decomposition and trunk biomass is a major contributor to stand-level biomass. It should be determined if, in mature stands without trunk fissures, lignomor contributes a significant amount of SOC.

The present work is part of the ongoing, worldwide purposeful activity to provide a foundation for addressing carbon emissions and sequestration associated with LUC or degradation of woody ecosystems.

Equations such as those developed here for mature-trees are necessary to quantify the C from primary-forests that humanity has historically relocated and how much it may relocate in the future. Those amounts form part of climate change modelling and national GHG accounting, and they correspond to the potential of re-sequestration projects to offset emissions. The present work has also:

1) provided formulae relating natural phenomena, to facilitate modelling carbon dynamics; e,g, the stand-level formulas with only large trees as the dependent variables will allow more field data collection with the same person-power in future studies on similar sites.
2) increased understanding of SOC distribution, e.g. development of a robust method to calculate cumulative SOC for a diverse soil profile;
3) encouraged a more discerning interpretation of literature reviews on LUC; and
4) raised the question of the impact of the Extra-SOC found in primary forests if climate change forces it to become a greenhouse gas emission.

Declaration of Competing Interest

The authors declare that they have no known competing financial interests or personal relationships that could have appeared to influence the work reported in this paper.

Acknowledgements

The authors are grateful to the following people: Thomas Rodemann at the University of Tasmania for operating the Elemental Analyser, David Green for help with fieldwork and soil laboratory work, John Gouzos of CSIRO, Adelaide for the inorganic C analysis, volunteers with The Wilderness Society for stand-level measurements of DBH and CWD, Michael Bosse and Robert Zlot for equipment and raw data processing of Zebedee mobile LiDAR, Melinda Lambourne for help with soil sampling, Patrick Dietrich for provision of his raw data, Mark Hovenden and Garth Oliver for use of their soil mill, and to the Editors and two anonymous reviewers for suggested improvements to the manuscript.

Funding

This work was supported in part by the University of Tasmania, including a Natural and Environmental Studies Elite Research Scholarship.

Appendix A. Supplementary data

Supplementary data to this article can be found online at https://doi.org/10.1016/j.geoderma.2020.114541.

References

Adkins, M.F., 2006. A burning issue: using fire to accelerate tree hollow formation in Eucalyptus species. Australian Forestry 69, 107–113. https://doi.org/10.1080/00049158.2006.10676236.

Allard, H.A., Leonard, E.C., 1952. The Canaan and Stoney River Valleys of West Virginia, their former magnificent spruce forest, their vegetation and floristics today. Castanea 17, 1–60.

ANM, 1959. The forests of the concession. Newsprint Log (Australian Newsprint Mills Pty. Ltd., Tasmania), 15, 21–25.

ANM, 1979. Working Plan For Concession Area Of Australian Newsprint Mills Limited In The Derwent Valley. Australian Newsprint Mills Limited, Boyer, Boyer, Tasmania, 45 pp.

Archer, D., et al., 2009. Atmospheric lifetime of fossil fuel carbon dioxide. Annu. Rev. Earth Planet. Sci. 37, 117–134. https://doi.org/10.1146/annurev.earth.031208.100206.

Ashton, D.H., 1975. The root and shoot development of *Eucalyptus regnans* F. Muell. Australian J. Botany 23, 867–887. https://doi.org/10.1071/BT9750867.

Ashton, D.H., 1981. Fire in tall open-forests (wet sclerophyll forests). In: A.M. Gill, R.H. Groves and I.R. Noble (Editors), Fire and the Australian Biota. Australian Academy of Science, Canberra, pp. 339–366.

Błońska, E., Lasota, J., Tullus, A., Lutter, R., Ostonen, I., 2019. Impact of deadwood decomposition on soil organic carbon sequestration in Estonian and Polish forests. Ann. Forest Sci. 76, 1–14. https://doi.org/10.1007/s13595-019-0889-9.

Bowman, D.M.J.S., Williamson, G.J., Keenan, R.J., Prior, L.D., 2014. A warmer world will reduce tree growth in evergreen broadleaf forests: evidence from Australian temperate and subtropical eucalypt forests. Glob. Ecol. Biogeogr. 23, 925–934. https://doi.org/10.1111/geb.12171.

Braakhekke, M.C., et al., 2013. Modeling the vertical soil organic matter profile using Bayesian parameter estimation. Biogeosciences 10, 399–420. https://doi.org/10.5194/bg-10-399-2013.

Bradshaw, C.J.A., et al., 2013. Brave new green world – consequences of a carbon economy for the conservation of Australian biodiversity. Biol. Conserv. 161, 71–90. https://doi.org/10.1016/j.biocon.2013.02.012.

Bruckner, A., Kandeler, E., Kampichler, C., 1999. Plot-scale spatial patterns of soil water content, pH, substrate-induced respiration and N mineralization in a temperate coniferous forest. Geoderma 83, 207–223. https://doi.org/10.1016/S0016-7061(99)00059-2.

Butt, N., Slade, E., Thompson, J., Malhi, Y., Riutta, T., 2013. Quantifying the sampling error in tree census measurements by volunteers and its effect on carbon stock estimates. Ecol. Appl. 23, 936–943. https://doi.org/10.1890/11-2059.1.

Canadell, J., et al., 1996. Maximum rooting depths of vegetation at the global scale. Oecologia 108, 583–595.

Caseldine, C.J., Hatton, J., 1993. The development of high moorland on Dartmoor: Fire and the influence of Mesolithic activity on vegetation change. In: F. Chambers (Editor), Climatic Change and Human Impact on the landscape: studies in palaeoecology and environmental archaeology. Chapman & Hall, London, pp. 119–131.

Commonwealth of Australia, 2018. Climate Data Online, Bureau of Meteorology, Available at: http://bom.gov.au/climate/data, [accessed: 02-January-2018].

Conant, R.T., Smith, G.R., Paustian, K., 2003. Spatial variability of soil carbon in forested and cultivated sites: implications for change detection. J. Environ. Qual. 32, 278–286. https://doi.org/10.2134/jeq2003.2780.

Cremer, K.W., 1962. The effect of fire on eucalypts reserved for seeding. Australian Forestry 26, 129–154. https://doi.org/10.1080/00049158.1962.10675921.

da Silva, W. and da Silva, C.P., 2015. LABFit Curve Fitting Software. v7.2.48, Brazil. Available at: http://zeus.df.ufcg.edu.br/labfit/, [accessed 28-October-2016]..

Dean, C., Fitzgerald, N.B., Wardell-Johnson, G.W., 2012a. Pre-logging carbon accounts in old-growth forests, via allometry: An example of mixed-forest in Tasmania, Australia. Plant Biosystems 146, 223–236. https://doi.org/10.1080/11263504.2011.638332.

Dean, C., Horn, E., 2019. A hard, high-carbon, lignomor with conchoidal fracture: cunnite, from mature myrtle beech (Nothofaus cunninghamii (Hook. f.) Oerst.). Geoderma, In Press, doi:10.1016/j.geoderma.2018.07.006.

Dean, C., Kirkpatrick, J.B., Friedland, A.J., 2017. Conventional intensive logging promotes loss of organic carbon from the mineral soil. Glob. Change Biol. 23, 1–11. https://doi.org/10.1111/gcb.13387.

Dean, C., et al., 2018. Novel 3D-geometry and models of the lower regions of large trees for use in carbon accounting of primary forests. AoB Plants 10, 1–19. https://doi.org/10.1093/aobpla/ply015.

Dean, C., Roxburgh, S.H., 2006. Improving visualisation of mature, high-carbon-sequestering forests. Forest Biometry, Modell. Inf. Sci. 1, 48–69.

Dean, C., et al., 2012b. Accounting for space and time in soil carbon dynamics in timbered rangelands. Ecol. Eng. 38, 51–64. https://doi.org/10.1016/j.ecoleng.2011.10.008.

Dean, C., Roxburgh, S.H., Mackey, B.G., 2003. Growth Modelling of Eucalyptus regnans for Carbon Accounting at the Landscape Scale. In: A. Amaro, D. Reed and P. Soares (Editors), Modelling Forest Systems. CABI Publishing, Wallingford, Oxford, U.K., pp. 27-39 + plates.

Dean, C., Roxburgh, S.H., Mackey, B.G., 2004. Forecasting landscape-level carbon sequestration using gridded, spatially adjusted tree growth. For. Ecol. Manage. 194, 109–129. https://doi.org/10.1016/j.foreco.2004.02.013.

Dean, C., Wardell-Johnson, G., 2010. Old-growth forests, carbon and climate change: functions and management for tall open-forests in two hotspots of temperate Australia. Plant Biosystems 144, 180–193. https://doi.org/10.1080/11263500903560751.

Dean, C., Wardell-Johnson, G.W., Kirkpatrick, J.B., 2012c. Are there any circumstances in which logging primary wet-eucalypt forest will not add to the global carbon burden? Agric. For. Meteorol. 161, 156–169. https://doi.org/10.1016/j.agrformet.2012.03.021.

di Folco, M.-B., Kirkpatrick, J.B., 2013. Organic soils provide evidence of spatial variation in human-induced vegetation change following European occupation of Tasmania. J. Biogeogr. 40, 197–205. https://doi.org/10.1111/j.1365-2699.2012.02779.x.

Dietrich, P., 2012. Carbon stocks in coarse woody debris and soil in the mixed forests and the rainforests in southern Tasmania. MSc Thesis, Technische Universität, Dresden, Germany..

Dixon, R.K., et al., 1994. Carbon pools and flux of global forest ecosystems. Science 263, 185–190. https://doi.org/10.1126/science.263.5144.185.

Døckersmith, I.C., Giardina, C.P., Sanford Jr., R.L., 1999. Persistence of tree related patterns in soil nutrients following slash-and-burn disturbance in the tropics. Plant Soil 209, 137–156. https://doi.org/10.1023/A:1004503023973.

Dubeux, J.C.B., Jr. et al., 2014. Soil characteristics under legume and non-legume tree canopies in signalgrass (Brachiaria decumbens) pastures. African J. Range Forage Sci., 31, 1–6.

Eby, M., et al., 2009. Lifetime of Anthropogenic climate change: millennial time scales of potential CO_2 and surface temperature perturbations. J. Clim. 22, 2501–2511.

Edney, P.A., Kershaw, A.P., De Decker, P., 1990. A Late Pleistocene and Holocene vegetation and environmental record from Lake Wangoom, Western Plains of Victoria, Australia. Palaeogeogr. Palaeoclimatol. Palaeoecol. 80, 325–343. https://doi.org/10.1016/0031-0182(90)90141-S.

Farjon, A., 2017. Ancient oaks in the English landscape. Royal Botanic Gardens, Kew, London.
Fedrigo, M., Kasel, S., Bennett, L.T., Roxburgh, S.H., Nitschke, C.R., 2014. Carbon stocks in temperate forests of south-eastern Australia reflect large tree distribution and edaphic conditions. For. Ecol. Manage. 334, 129–143. https://doi.org/10.1016/j.foreco.2014.08.025.
Ferguson, K.V.M., 1948. Some statistics of timber yields from virgin stands of white mountain ash. Australian Forestry 12, 13–15. https://doi.org/10.1080/00049158.1948.10675264.
Finzi, A.C., Van Breemen, N., Canham, C.D., 1998. Canopy tree–soil interactions within temperate forests: species effects on soil carbon and nitrogen. Ecol. Appl. 8, 440–446. https://doi.org/10.1890/1051-0761(1998)008[0440:CTSIWT]2.0.CO;2.
Galbraith, A.V., 1937. Mountain Ash (Eucalyptus regnans F. van Mueller): a General Treatise on its Silviculture, Management, and Utilization. Government Printer, Melbourne, 51 pp.
Galbraith, A.V., 1939. The disastrous forest fires of January 1939, in Victoria. Empire Forestry J. 18, 10–18.
García-Oliva, F., Lancho, J.F.G., Montañ, N.M., Islas, P., 2006. Soil Carbon and nitrogen dynamics followed by a forest-to-pasture conversion in western Mexico. Agrofor. Syst. 66, 93–100. https://doi.org/10.1007/s10457-005-2917-z.
Gifford, R.M., Roderick, M.L., 2003. Soil carbon stocks and bulk density: spatial or cumulative mass coordinates as a basis of expression? Glob. Change Biol. 9, 1507–1514. https://doi.org/10.1046/j.1529-8817.2003.00677.x.
Gilbert, J.M., 1959. Forest succession in the Florentine Valley, Tasmania. papers and Proceedings of the Royal Society of Tasmania, 93, 129–151.
Green, R.N., Trowbridge, R.L., Klinka, K., 1993. Towards a taxonomic classification of humus forms. Forest Sci., Monograph 29, 1–49.
Guo, L.B., Gifford, R.M., 2002. Soil carbon stocks and land use change: a meta analysis. Glob. Change Biol. 8, 345–360. https://doi.org/10.1046/j.1354-1013.2002.00486.x.
Hansen, M.C., et al., 2013. High-resolution global maps of 21st-century forest cover change. Science 342, 850–853. https://doi.org/10.1126/science.1244693.
Hararuk, O., Xia, J. and Yiqi Luo1, 2014. Evaluation and improvement of a global land model against soil carbon data using a Bayesian Markov chain Monte Carlo method. Journal of Geophysical Research: Biogeosciences, 119, 403–417, doi:10.1002/2013JG002535.
Harmon, M.E., 2001. Carbon sequestration in forests. Addressing the scale question. J. Forest. 99, 24–29.
Harmon, M.E., et al., 1986. Ecology of coarse woody debris in temperate ecosystems. Adv. Ecol. Res. 34, 133–302. https://doi.org/10.1016/S0065-2504(03)34002-4.
Harper, R.J., Tibbett, M., 2013. The hidden organic carbon in deep mineral soils. Plant Soil 368, 641–648. https://doi.org/10.1007/s11104-013-1600-9.
Harrison, R.B., et al., 2003. Quantifying deep-soil and coarse-soil fractions: avoiding sampling bias. Soil Sci. Soc. Am. J. 67, 1602–1606. https://doi.org/10.2136/sssaj2003.1602.
Harrison, R.B., Footen, P.W., Strahm, B.D., 2011. Deep soil horizons: contribution and importance to soil carbon pools and in assessing whole-ecosystem response to management and global change. Forest Sci. 57, 67–76.
Havlicek, E., Mitchell, E.A.D., 2014. Soils Supporting Biodiversity. In: J. Dighton and J.A. Krumins (Editors), Interactions in Soil: Promoting Plant Growth Biodiversity, Community and Ecosystems. Springer, Netherlands, pp. 27–58.
He, F., et al., 2014. Simulating global and local surface temperature changes due to Holocene anthropogenic land cover change. Geophys. Res. Lett. 41, 623–631. https://doi.org/10.1002/2013GL058085.
Heath, L.S., et al., 1993. Contribution of temperate forests to the world's carbon budget. Water Air and Soil Pollut. 70, 50–69. https://doi.org/10.1007/BF01104988.
Herrmann, W., 2006. Vulnerability of Tasmanian giant trees. Australian Forestry 69, 285–298. https://doi.org/10.1080/00049158.2006.10676249.
Hibbard, K.A., Schimel, D.S., Archer, S., Ojima, D.S., Parton, W., 2003. Grassland to woodland transitions: integrating changes in landscape structure and biogeochemistry. Ecol. Appl. 13, 911–926.
Hickey, J.E., Kostoglou, P., Sargison, G.J., 2000. Tasmania's tallest trees. Tasforests 12, 105–122.
Hiederer, R., Köchy, M., 2011. Global Soil Organic Carbon Estimates and the Harmonized World Soil Database. JRC Scientific and Technical Reports. Publications Office of the European Union, Luxembourg, 79 pp.
Hoffman, B.S.S., Anderson, R.S., 2014. Tree root mounds and their role in transporting soil on forested landscapes. Earth Surf. Proc. Land. 39, 711–722. https://doi.org/10.1002/esp.3470.
Houghton, J., 1997. Global Warming: The Complete Briefing. Cambridge University Press, Cambridge, England.
Houghton, J.T., et al., 1994. Climate Change 1994: Radiative Forcing of Climate Change and an Evaluation of the 1992 IPCC IS92 Emissions Scenario. Cambridge University Press, Cambridge, 339 pp.
Houghton, R.A., et al., 2012. Carbon emissions from land use and land-cover change. Biogeosciences 9, 5125–5142. https://doi.org/10.5194/bg-9-5125-2012.
House, J.I., Prentice, I.C., Le Quéré, C., 2002. Maximum impacts of future reforestation or deforestation on atmospheric CO_2. Glob. Change Biol. 8, 1047–1052. https://doi.org/10.1046/j.1365-2486.2002.00536.x.
Huntington, T.G., Johnson, C.E., Johnson, A.H., Siccama, T.G., Ryan, D.F., 1989. Carbon, organic matter, and bulk density relationships in a forested spodosol. Soil Sci. 148, 38–386.
IPCC, 2003. LUCF Sector Good Practice Guidance. In: J. Penman et al. (Editors), IPCC Good practice guidance for land use, land-use change and forestry. National Greenhouse Gas Inventories Programme Technical Support Unit, Institute for Global Environmental Strategies, Hayama, Kanagawa, Japan.
Jacob, M., et al., 2013. Significance of over-mature and decaying trees for carbon stocks in a central European natural spruce forest. Ecosystems 16, 336–346. https://doi.org/10.1007/s10021-012-9617-0.
James, J., Devine, W., Harrison, R., Terry, T., 2014. Deep Soil Carbon: Quantification and Modeling in Subsurface Layers. Soil Sci. Soc. Am. J. 78, S1. https://doi.org/10.2136/sssaj2013.06.0245nafsc.
Jobággy, G.J., Jackson, R.B., 2002. The vertical distribution of soil organic carbon and its relation to climate and vegetation. Ecol. Appl. 10, 423–436. https://doi.org/10.2307/2641104.
Johnson, M.S., et al., 2008. CO_2 efflux from Amazonian headwater streams represents a significant fate for deep soil respiration. Geophys. Res. Lett. 35. https://doi.org/10.1029/2008GL034619.
Jurgensen, M.F., et al., 1997. Impacts of timber harvesting on soil organic matter, nitrogen, productivity, and health of inland Northwest forests. Forest Sci. 43, 234–251.
Kaplan, J.O., et al., 2010. Holocene carbon emissions as a result of anthropogenic land cover change. Holocene 21, 775–791. https://doi.org/10.1177/0959683610386983.
Kashian, D.M., Romme, W., Tinker, D.B., Turner, M.G., Ryan, M.G., 2006. Carbon storage on landscapes with stand-replacing fires. Bioscience 56, 598–606. https://doi.org/10.1641/0006-3568(2006)56[598:CSOLWS]2.0.CO;2.
Kauppi, P.E., et al., 2015. Effects of land management on large trees and carbon stocks. Biogeosciences 12, 855–862. https://doi.org/10.5194/bg-12-855-2015.
Keith, H., Mackey, B.G., Lindenmayer, D.B., 2009. Re-evaluation of forest biomass carbon stocks and lessons from the world's most carbon-dense forests. PNAS 106, 11635–11640. https://doi.org/10.1073/pnas.0901970106.
Khomo, L., Trumbore, S., Bern, C.R., Chadwick, O.A., 2017. Timescales of carbon turnover in soils with mixed crystalline mineralogies. Soil 3, 17–30. https://doi.org/10.5194/soil-3-17-2017.
Kirkpatrick, J.B., 1986. Some ecological aspects of forest conservation in temperate Australia. In: Y. Hanxi, W. Zhan, J.N.R. Jeffers and P.A. Ward (Editors), International Symposium on Temperate Forest Ecosystem Management and Environmental Protection. Institute of Terrestrial Ecology, Natural Environment Research Council, Changbai Mountain Research Station Academia Sinica Antu, Jilin Province, People's Republic of China, pp. 68–77.
Kirkpatrick, J.B., 1994. A Continent Transformed. Human Impact on the Natural Vegetation of Australia. Oxford University Press, Melbourne, 144 pp.
Kirkpatrick, J.B. and DellaSala, D.A., 2011. Temperate Rainforests of Australasia. In: D.A. DellaSala (Editor), Temperate and Boreal Rainforests of the World: Ecology and Conservation. Island Press, Washington DC, pp. 195-212.
Kirkpatrick, J.B., Peacock, R.J., Cullen, P.J. and Neyland, M.G., 1988. The Wet Eucalypt Forests of Tasmania. Tasmanian Conservation Trust Hobart, Hobart.
Kirschbaum, M.U.F., 2004. Soil respiration under prolonged soil warming: are rate reductions caused by acclimation or substrate loss? Glob. Change Biol. 10, 1870–1877. https://doi.org/10.1111/j.1365-2486.2004.00852.x.
Kolchugina, T.P., Vinson, T.S., 1995. Role of Russian Forests in the Global Carbon Balance. Ambio 24, 258–264.
Laurance, W.F., Delamônica, P., Laurance, S.G., Vasconcelos, H.L., Lovejoy, T.E., 2000. Rainforest fragmentation kills big trees. Nature 404, 836.
Levia Jr., D.F., Frost, E.E., 2003. A review and evaluation of stemflow literature in the hydrologic and biogeochemical cycles of forested and agricultural ecosystems. J. Hydrol. 274, 1–29.
Lindbladh, M., Fraver, S., Edvardsson, J., Felton, A., 2013. Past forest composition, structures and processes – How paleoecology can contribute to forest conservation. Biol. Conserv. 168, 116–127. https://doi.org/10.1016/j.biocon.2013.09.021.
Lindenmayer, D.B., Laurance, W.F., Franklin, J.F., 2012. Global decline in large old trees. Science 1305. https://doi.org/10.1126/science.1231070.
Liski, J., 1995. Variation in soil organic carbon and thickness of soil horizons within a boreal forest stand- effect of tree and implications for sampling. Silva Fennica 29, 255–266.
Lodge, D.J., Winter, D., González, G., Clum, N., 2016. Effects of hurricane-felled tree trunks on soil carbon, nitrogen, microbial biomass, and root length in a wet tropical forest. Forests 7, 1–19. https://doi.org/10.3390/f7110264.
Luo, Y., Keenan, T.F., Smith, M., 2015. Predictability of the terrestrial carbon cycle. Glob. Change Biol. 21, 1737–1751. https://doi.org/10.1111/gcb.12766.
Lutz, H.J., 1960. Fire As an ecological factor in the boreal forest of Alaska. J. Forestry 58, 454–460. https://doi.org/10.1093/jof/58.6.454.
MacFie, P., 1999. Maydena, the logging town in a colonised valley. In: J. Dargavel and B. Libbis (Editors), Australia's Ever-Changing Forests IV. Proceedings of the Fourth National Conference on Australian Forest History. Australian National University & Australian Forest History Society Inc., Canberra, pp. 293-308.
Mackey, B., et al., 2015. Policy options for the world's primary forests in multilateral environmental agreements. Conserv. Lett. 8, 139–147. https://doi.org/10.1111/conl.12120.
McIntyre, P.J., et al., 2015. Twentieth-century shifts in forest structure in California: denser forests, smaller trees, and increased dominance of oaks. PNAS 112, 1458–1463. https://doi.org/10.1073/pnas.1410186112.
Metz, J., 2009. Deforestation. In: K. R. and T. N. (Editors), International Encyclopaedia of Human Geography. Elsevier, Oxford, pp. 39–50.
Mobley, M.L., Richter, D.D., Heine, P.R., 2013. Accumulation and decay of woody detritus in a humid subtropical secondary pine forest. Can. J. For. Res. 43, 109–118. https://doi.org/10.1139/cjfr-2012-0222.
Mount, A.B., 1964. Three Studies in Forest Ecology, University of Tasmania, 145 pp.
MRT, 2011. Tasmania. Geology 1:25,000. Mineral Resources of Tasmania, Hobart, Tasmania.
Murty, D., Kirschbaum, M.U.F., McMurtrie, R.E., Mcgilvray, H., 2002. Does conversion of forest to agricultural land change soil carbon and nitrogen? a review of the literature. Glob. Change Biol. 8, 105–123. https://doi.org/10.1046/j.1354-1013.2001.00459.x.
Ngo, K.M., et al., 2013. Carbon stocks in primary and secondary tropical forests in

Singapore. For. Ecol. Manage. 296, 81–89.
Olofsson, J., Hickler, T., 2008. Effects of human land-use on the global carbon cycle during the last 6,000 years. Veget. History Archaeobotany 17, 605–615. https://doi.org/10.1007/s00334-007-0126-6.
Ostle, N.J., et al., 2009. Integrating plant–soil interactions into global carbon cycle models. J. Ecol. 07, 851–863. https://doi.org/10.1111/j.1365-2745.2009.01547.x.
Oyarzún, C.E., Godoy, R., Staelens, J., Donoso, P.J., Verhoest, N.E.C., 2011. Seasonal and annual throughfall and stemflow in Andean temperate rainforests. Hydrol. Process. 25, 623–633. https://doi.org/10.1002/hyp.7850.
Paul, E.A., 2016. The nature and dynamics of soil organic matter: Plant inputs, microbial transformations, and organic matter stabilization. Soil Biol. Biochem. 109–126. https://doi.org/10.1016/j.soilbio.2016.04.001.
Périeé, C., Ouimet, R., 2008. Organic carbon, organic matter and bulk density relationships in boreal forest soils. Can. J. Soil Sci. 88, 315–325. https://doi.org/10.4141/CJSS06008.
Phillips, J.D., Marion, D.A., 2005. Biomechanical effects, lithological variations, and local pedodiversity in some forest soils of Arkansas. Geoderma 124, 73–89. https://doi.org/10.1016/j.geoderma.2004.04.004.
Pinter, N., Fiedel, S., Keeley, J.E., 2011. Fire and vegetation shifts in the Americas at the vanguard of Paleoindian migration. Quat. Sci. Rev. 30, 269–272. https://doi.org/10.1016/j.quascirev.2010.12.010.
Polglase, P.J., Adams, M.A. and Attiwill, P.M., 1994. Measurement and Modelling of Carbon Storage in a Chronosequence of Mountain Ash Forests: Implications for Regional and Global Carbon Budgets. State Electricity Commission, Melbourne, Victoria, Australia, 62 pp.
Prescott, C.E., Grayston, S.J., 2013. Tree species influence on microbial communities in litter and soil: current knowledge and research needs. For. Ecol. Manage. 309, 19–27. https://doi.org/10.1016/j.foreco.2013.02.034.
Rafelski, L.E., Piper, S.C., Keeling, R.F., 2009. Climate effects on atmospheric carbon dioxide over the last century. Tellus 61B, 718–731. https://doi.org/10.1111/j.1600-0889.2009.00439.x.
Raich, J.W., Schlesinger, W.H., 1992. The global carbon dioxide flux in soil respiration and its relationship to vegetation and climate. Tellus 44B, 81–99. https://doi.org/10.1034/j.1600-0889.1992.t01-1-00001.x.
Rankin, M.A., 1947. Reforestation. Newsprint Log. Australian Newsprint Mills Pty. Ltd., pp. 1–11 2.
Raupach, M., Tucker, B.M., 1959. The field determination of soil pH reaction. J. Austral. Institute Agric. Sci. 25, 129–133.
Rayment, G.E. and Lyons, D.J., 2011. Soil pH, Soil Chemical Methods-Australasia. CSIRO, Collingwood, VIC, Australia, pp. 33–48.
Rhemtulla, J.M., Mladenoff, D.J., Clayton, M.K., 2009. Historical forest baselines reveal potential for continued carbon sequestration. PNAS 106, 6082–6087. https://doi.org/10.1073/pnas.0810076106.
Richter, D.D., Oh, N.-H., Fimmen, R. and Jackson, J., 2007. The Rhizosphere and Soil Formation. In: Z.G. Cardon and J.L. Whitbeck (Editors), The Rhizosphere. An Ecological Perspective. Elsevier, Amsterdam, pp. 179–200.
Rossetti, I., et al., 2015. Isolated cork oak trees affect soil properties and biodiversity in a Mediterranean wooded grassland. Agric. Ecosyst. Environ. 202, 203–216. https://doi.org/10.1016/j.agee.2015.01.008.
Roxburgh, S.H., et al., 2006. Organic carbon partitioning in soil and litter in subtropical woodlands and open forests: a case study from the Brigalow Belt, Queensland. Rangeland J. 28, 115–125. https://doi.org/10.1071/rj05015.
Royer, D.L., 1999. Depth to pedogenic carbonate horizon as a paleoprecipitation indicator? Geology 27, 1123–1126.
Rudiman, W.F., 2003. The anthropogenic greenhouse era began thousands of years ago. Clim. Change 61, 261–293. https://doi.org/10.1023/B:CLIM.00000.
Rumpel, C., Kögel-Knaber, I., 2010. Deep soil organic matter—a key but poorly understood component of terrestrial C cycle. Plant Soil 338, 143–158. https://doi.org/10.1007/s11104-010-0391-5.
Ryan, K.C., Frandsen, W.H., 1991. Basal injury from smoldering fires in mature *Pinus ponderosa* Laws. Int. J. Wildland Fire 1, 107–118. https://doi.org/10.1071/WF9910107.
Saetre, P., Bååth, E., 2000. Spatial variation and patterns of soil microbial community structure in a mixed spruce-birch stand. Soil Biol. Biochem. 32, 909–917. https://doi.org/10.1016/S0038-0717(99)00215-1.
Salinger, M.J., 2007. Agriculture's influence on climate during the Holocene. Agric. For. Meteorol. 142, 96–102. https://doi.org/10.1016/j.agrformet.2006.03.024.
Šamonil, P., Daněk, P., Senecká, A., Adam, D., Phillips, J.D., 2018. Biomechanical effects of trees in an old-growth temperate forest. Earth Surf. Proc. Land. 43, 1063–1072. https://doi.org/10.1002/esp.4304.
Schaetzl, R. and Thompson, m.L., 2005. Soils: Genesis and Geomorphology. Cambridge University Press, Cambridge, 817 pp.
Scharlemann, J.P.W., Tanner, E.V.J., Hiederer, R., Kapos, V., 2014. Global soil carbon: understanding and managing the largest terrestrial carbon pool. Carbon Manage. 5, 81–91. https://doi.org/10.4155/cmt.13.77.
Schöning, I., Totsche, K.U., Kögel-Knabner, I., 2006. Small scale spatial variability of organic carbon stocks in litter and solum of a forested Luvisol. Geoderma 136, 631–642. https://doi.org/10.1016/j.geoderma.2006.04.023.
Sillett, S.C., et al., 2018. Manipulating tree crown structure to promote old-growth characteristics in second-growth redwood forest canopies. For. Ecol. Manage. 417, 77–89. https://doi.org/10.1016/j.foreco.2018.02.036.
Sillett, S.C., Bailey, M.G., 2003. Effects of tree crown structure on biomass of the epiphytic fern *Polypodium scouleri* (Polypodiaceae) in redwood forests. Am. J. Bot. 90, 255–261. https://doi.org/10.3732/ajb.90.2.255.
Sillett, S.C., et al., 2019. Allometric equations for *Sequoia sempervirens* in forests of different ages. For. Ecol. Manage. 433, 349–363. https://doi.org/10.1016/j.foreco.2018.11.016.
Sillett, S.C., Van Pelt, R., 2007. Trunk reiteration promotes epiphytes and water storage in an old-growth redwood forest canopy'. Ecol. Monogr. 77, 335–359. https://doi.org/10.1890/06-0994.1.
Sillett, S.C., et al., 2010. Increasing wood production through old age in tall trees. For. Ecol. Manage. 259, 976–994. https://doi.org/10.1016/j.foreco.2009.12.003.
Sillett, S.C., Van Pelt, R., Kramer, R.D., Carroll, A.L., Koch, G.W., 2015. Biomass and growth potential of *Eucalyptus regnans* up to 100 m tall. For. Ecol. Manage. 348, 78–91. https://doi.org/10.1016/j.foreco.2015.03.046.
Silvester, W.B., Orchard, T.A., 1999. The biology of kauri (Agathis australis) in New Zealand. Production, biomass, carbon storage, and litter fall in four forest remnants. N. Z. J. Botan. 37, 553–571.
Slik, J.W.F., et al., 2013. Large trees drive forest aboveground biomass variation in moist lowland forests across the tropics. Glob. Ecol. Biogeogr. 22, 1261–1271. https://doi.org/10.1111/geb.12092.
Strukelj, M., et al., 2013. Chemical transformations in downed logs and snags of mixed boreal species during decomposition. Can. J. For. Res. 43, 785–798. https://doi.org/10.1139/cjfr-2013-0086.
Sucre, E.B. and Fox, T.R., 2008. Contribution of stumps to carbon and nitrogen pools in southern Appalachian hardwood forests. In: D.F.J.C.H. Michler (Editor), 16th Central Hardwood Forest Conference. Department of Agriculture, Forest Service, Northern Research Station, West Lafayette, IN, USA, pp. 233–239.
Sucre, E.B., Fox, T.R., 2009. Decomposing stumps influence carbon and nitrogen pools and fine-root distribution in soils. For. Ecol. Manage. 258, 2242–2248 doi:j.-foreco.2009.05.012.
Thomas, S.C., Martin, A.R., 2012. Carbon content of tree tissues: a synthesis. Forests 3, 332–352. https://doi.org/10.3390/f3020332.
Thompson, I., Mackey, B.G., McNulty, S. and Mosseler, A., 2009. Forest Resilience, Biodiversity, and Climate Change. A Synthesis of the Biodiversity/Resilience/Stability Relationship in Forest Ecosystems. Secretariat of the Convention on Biological Diversity, Montreal, 67 pp.
Throop, H.L., Archer, S.R., 2008. Shrub (*Proposis velutina*) encroachment in a semidesert grassland: spatial-temporal changes in organic carbon and nitrogen pools. Glob. Change Biol. 14, 1–12. https://doi.org/10.1111/j.1365-2486.2008.01650.x.
Tipping, E., Chamberlain, P.M., Froberg, M., Hanson, P.J., Jardine, P.M., 2012. Simulation of carbon cycling, including dissolved organic carbon transport, in forest soil locally enriched with 14C. Biogeochemistry 108, 91–107. https://doi.org/10.1007/s10533-011-9575-1.
Trumbore, S., 2009. Radiocarbon and soil carbon dynamics. Annu. Rev. Earth Planet. Sci. 37, 47–66 0.1146/annurev.earth.36.031207.124300.
Turner, P.A.M., Balmer, J., Kirkpatrick, J.B., 2009. Stand-replacing wildfires? The incidence of multicohort and single-cohort Eucalyptus regnans and E. obliqua forests in southern Tasmania. For. Ecol. Manage. 258, 366–375. https://doi.org/10.1016/j.foreco.2009.04.021.
Wagg, C., Bender, S.F., Widmer, F., van der Heijden, M.G.A., 2014. Soil biodiversity and soil community composition determine ecosystem multifunctionality. PNAS 111, 5266–5270. https://doi.org/10.1073/pnas.1320054111.
Warszawski, L., et al., 2013. A multi-model analysis of risk of ecosystem shifts under climate change. Environ. Res. Lett. 8, 044018. https://doi.org/10.1088/1748-9326/8/4/044018.
Warton, D.I., Wright, I.J., Falster, D.J., Westoby, M., 2006. Bivariate line-fitting methods for allometry. Biol. Rev. (Cambridge) 81, 259–291. https://doi.org/10.1017/S1464793106007007.
Wendt, J.W., Hauser, S., 2013. An equivalent soil mass procedure for monitoring soil organic carbon in multiple soil layers. Eur. J. Soil Sci. 64, 58–65. https://doi.org/10.1111/ejss.12002.
Wilde, S.A., 1946. Forest Soils and Forest Growth. Chronica Botanica Company, Waltham, Mass. USA, 22-24 pp.
Williams, C.B., Sillett, S.C., 2007. Epiphyte communities on redwood (Sequoia sempervirens) in northwestern California. Bryologist 110, 420–452.
Wilson, B.R., Moffat, A.J., Nortcliff, S., 2010. The nature of three ancient woodland soils in southern England. J. Biogeogr. 24, 633–646. https://doi.org/10.1111/j.1365-2699.1997.tb00074.x.
Wirth, C., Gleixner, G. and Heimann, M., 2009. Old-Growth Forests: Function, Fate and Value – an Overview. Ecological Studies 207. Springer-Verlag, Heidleberg, 512 pp.
Wood, S.W., Hua, Q., Allen, K.J., Bowman, D.J.M.S., 2010. Age and growth of a fire prone Tasmanian temperate old-growth forest stand dominated by *Eucalyptus regnans*, the world's tallest angiosperm. For. Ecol. Manage. 260, 438–447. https://doi.org/10.1016/j.foreco.2010.04.037.
Wooley, L.P., Henkel, T.W., Sillett, S.C., 2008. Reiteration in the monodominant tropical tree *Dicymbe corymbosa* (Caesalpiniaceae) and its potential adaptive significance. Biotropica 40, 32–43. https://doi.org/10.1111/j.1744-7429.2007.00348.x.
Zabowski, D., Whitney, N., Gurung, J., Hatten, J., 2011. Total soil carbon in the coarse fraction and at depth. Forest Sci. 57, 11–18.

Supporting Information for

The overlooked soil carbon under large, old trees

Christopher Dean[a,*], Jamie B. Kirkpatrick[a], Richard B. Doyle[b], Jon Osborn[a], Nicholas B. Fitzgerald[a] and Stephen H. Roxburgh[c]

[a]School of Technology, Environments and Design, University of Tasmania, Private Bag 78, Hobart, TAS 7001, Australia.

[b]Tasmanian Institute of Agriculture, University of Tasmania, Private Bag 98, Hobart, TAS 7001, Australia.

[c]CSIRO Land & Water, GPO Box 1700, Canberra ACT 2601, Australia.

[*] Corresponding author, email: christopher.dean@utas.edu.au, cdeanspace@gmail.com, +61-(0)408-975-633

https://doi.org/10.1016/j.geoderma.2020.114541

1. Supporting Introduction

The Supporting Information is presented mainly to explain the more-typical soil data processing methods, and to compare them with the new method that we described in the text, called 'M4' herein, designed for soil profiles under tree trunks and their surrounds.

We also compare the observed CWD decomposition stages with those in the literature and describe our procedure to derive the 'soil wood' or lignomor component.

This Supporting Information also includes fine detail for the Methods section and Discussion section as an adjunct to the main text, plus a table of 50 tree species other than *Eucalyptus regnans* that may have under-trunk lignomor when mature.

2. Supporting Methods

2.1 Study area

Trend detection of the study site's climate

Using a Mann-Kendall test for trend detection and Sen's slope calculation (Salmi et al., 2002) there was a decrease in annual rainfall of 1.6 mm/year from 1974–2017 (confidence level: alpha= 0.05), mostly in autumn and summer, but with an increasing late-winter maximum. Over the last 60 years the average monthly minimum and maximum temperatures have increased by 0.023 ºC/year and 0.024 ºC/year respectively (confidence level: alpha= 0.01), with the increases being most consistent in winter.

Effect of fire on the major carbon pools, species distribution and age structure

The fire severity and frequency in the study region relate to carbon stock by determining the tree species and size, the depth and longevity of the humus layer, and the size and longevity of logs on the ground (Ashton, 1981; Cremer, 1962; Gilbert, 1959). The eucalypt stands can be killed by severe wildfire, after which an even-aged stand of *E. regnans* grows. The rainforest understorey is uneven-aged but its oldest members can be older than the eucalypts. Some of the forest stands in the region were uneven-aged, due to less-severe wildfires (Turner et al., 2009). In moist gullies and depressions, where fire is far less-frequent (e.g. once every 1,000 years), there are no eucalypts. If severe fire is too frequent then mixed-forest is replaced by wet-sclerophyll forest (Kirkpatrick et al., 1988), which is likely to be less carbon rich.

2.2 Inorganic C analysis

Inorganic C analysis followed the method of Sherrod et al. (2002) and Rayment and Lyons (2011) and was performed by John Gouzos of CSIRO, Adelaide. Inorganic C was determined by reacting the sample with acid in a sealed container and measuring the pressure increase. An amount of finely ground sample, sufficient to contain no more than 0.8 g $CaCO_3$ equivalent was weighed into a 250 mL glass bottle, a tube containing 8 mL 3*M* HCl and 3% ferrous chloride added and the bottle sealed. The contents were mixed intermittently during a

one hour period and the pressure in the bottle measured by piercing the septum with a needle attached to a pressure transducer.

2.3 SOC data processing

2.3.1 Method 1 (M1): Where SOC density can be expressed as a mathematical function of depth, the cumulative carbon per unit area can be calculated by analytical integration of the function from 0 m to a particular depth (e.g. Jobággy and Jackson, 2002), or to minus infinity to give the cumulative carbon for the [whole] mineral soil (Ogawa et al., 1961). Infinity is an approximation to include a fractured C horizon, with its heterogeneity and some SOC in the form of dissolved organic carbon (DOC). The simple exponential decay function for SOC density:

$$SOC\_density = a[\exp(cz)] \qquad \text{Supporting Eq1}$$

where z is the distance from the solum surface (in metres, negative below 0 m) and *SOC_density* is in kg·m^{-3}, appears to have been used first by Ogawa et al. (1961). Its integral:

$$cumulative\_SOC = (10a/c)[1 - \exp(cz)] \qquad \text{Supporting Eq2}$$

where *cumulative_SOC* is in Mg·ha^{-1}, gives the cumulative unit-area SOC with depth (Mishra et al., 2009; Ogawa et al., 1961; Roxburgh et al., 2006). This is an approximation as contrasting soil horizons are likely to cause vacillations in the slope of cumulative SOC/depth. Thus the change in SOC density with depth is unlikely to be a simple exponential function over the whole soil profile and may even be non-monotonic, due to *inter alia* different properties of horizons (Kempen et al., 2011; Waksman, 1936). It was used here as a first approximation.

2.3.2 Method 2 (M2): Where the formula for SOC density as a function of depth is too complex to integrate analytically (e.g. 'trapezoidal' integration), the density values can be used to approximate the unit area stock for small depth intervals (e.g. 0.001 m), i.e. per

hectare, and these tallied by numerical integration over depth. For SOC concentration as a function of depth, and for cumulative SOC, several equations were tried, as suggested by the program Eureqa (Schmidt and Lipson, 2009) and were considered stable in nonlinear regression analyses (Ratkowsky, 1990). However, they had large error margins and the data were not of sufficient precision or uniformity to warrant the complex equations that best matched our soil profiles and therefore M2 was not further used.

2.3.3 Method3 (M3): The SOC density can be measured for specific broad layers of soil that may correspond to soil from visually different 'horizons', or to depth-spans measurable by specific technology. Measurements within each layer are averaged, then the depth-span of each layer is applied to give a unit area of measurement for those layers, and the layers' values summed. This method is commonly used to report results down to a specific depth, e.g. previously for *E. regnans*-dominated forests (Dietrich, 2012; Polglase et al., 1994) but care must be taken not to interpret that SOC stock as if referring to the whole profile. Method M3 was inapplicable to the soil structure in the present work because layers were often not visible under trees, and therefore it was not used.

2.3.4 Method 4 (M4): Method 4, which is the new method devised in the present work, is described in the main text, in Section 2.4 'SOC data processing'.

2.3.5 Application of the data processing methods

The method entitled 'fixed-C0' in the main text is 'M4-fixed C0' here in the Supporting Information.

Nonlinear regression played a larger part in determining the parameters for M1 than for M4 due to the greater spread of data for M1, and the uneven data point distribution [with depth] for M1 may have biased its derivation by regression. The 95% confidence intervals for M4 were relatively narrow because of the dependency of deeper SOC data on shallower data in M4, and therefore the variability of the deeper data is occluded in M4.

In the final analysis SOC was calculated by M1 and M4 only. M4 was considered to be the most accurate and M1 is that most commonly used in the literature. Equations for M1 and M4 were fitted to three main regions: under-trunk, under-humus (under the humus mound), and in between trees, the latter based on data from Dietrich (2012).

2.4 SOC in well-decomposed logs, 'soft-logs'

It was necessary to consider at what stage CWD becomes soil and therefore tallied with other SOC. For this purpose the chemical and physical attributes of CWD in common Canadian species (Strukelj et al., 2013) were compared with those for the under-trunk lignomor found in the present work. (There are no similar data for Australian cool-temperate forests.) In a five-category decay-class system the two most decayed, IV and V, are known as 'soil wood' (Jurgensen et al., 1997). A three-category classification system was used in the present work for CWD (hard, medium and soft). It was necessary to consider which of our decay classes matched 'soil wood' in order to tally that SOC at the stand-level.

The attributes of the lignomor: bulk density, SOC density and C/N ratio (Table 1), were within one standard deviation of those of 'decay class-V' of the Canadian CWD (186.20(21.2), 95.27(13.1) and 197.00(97.5) respectively (standard deviations from their reported data)). The colour of decay class-V in northern-USA forests is red-brown to dark-brown and has virtually no visible wood structure (Maser et al., 1979; McFee and Stone, 1966). This matches with the characteristics of *E. regnans* lignomor (red-brown) and some myrtle lignomor (dark-brown, though light-brown to orange-yellow in some trees), although fresh lignomor was yellow to orange but changed to red-brown to dark-brown or black once the fungal hyphae had died.

The 'decay class-IV' of Strukelj et al. (2013) had too high a C/N ratio to match the lignomor observed here. The C/N ratio was the elemental composition attribute of CWD with the highest standard deviation (close to 50%) in both the present study and in Strukelj et al.

(2013), this being due to the steep decline with decomposition, the patchy nature of decomposition stage within a cross-section of timber and possibly also due to variability between species of live wood. Different tree species sampled in the present study varied significantly in C/N (by up to five times).

Due to the similarities we considered that our 'soft' category corresponded to the 'decay class V' and some 'decay class IV' of Strukelj et al. (2013) and Grove et al. (2011). Grove et al. (2011 Fig. 3) found ~30–35% of decay classes IV plus V to be non-rotten wood in *E. obliqua* forest.

Therefore it seemed conservative, in relation to the idea that there is more SOC in the forest than indicated by between tree soil sampling, to suggest that half of the soft-log mass (in the present work) is equivalent to 'decay class V' and therefore is SOC rather than wood.

2.5 Minor SOC pools not tallied

Aboveground lignomor ($z>0$ m) in the trunk hollows, was not included in the stand-level tally (Figs 5.a, 7.b (main text)). The amount of this lignomor pool could not be readily measured but an estimate showed that 26 large trees per hectare containing lignomor up to 1.3 m in their trunk hollows would be required to increase the SOC per unit area by 1%. Only a few such trees were noted in each logged coupe. This low frequency may be because the lignomor has a much shorter half-life than the remaining timber around it, which persists for several hundred years, or because it had been dispersed by logging. The half-life would be shorter with a basal stem fissure.

A subset of the aboveground lignomor in hollows was cunnite (Dean and Horn, 2019), which was found only in mature myrtle trees. Cunnite is a dark, hard material, a dehydrated form of its wet precursor called cunncaseus, which is light coloured (Fig 5.b (main text)). Both cunnite and cunncaseus have conchoidal fracture which makes them readily discernible from other substances in the forest (Dean and Horn, 2019). The amount of C in cunnite and cunncaseus at the stand-level was probably two orders of magnitude less than that of the below-ground SOC.

In some trees in the non-decomposed heartwood-to-sapwood region of the buttress, between the central hollow and the bark, the sides of the neighbouring spurs had grown towards each other and compacted the flute, i.e. they had filled the previous inter-spur void. Over time the bark inclusions trapped within the wood had decomposed to form a peaty soil (e.g. Figs 5.c, 5.d (main text)) and in some places it included coarse and fine living roots of epiphytes. This soil was considered of negligible mass per hectare and not tallied in the stand-level accounts.

2.6 Stand-level effects

Tallying at the stand level was performed as described in the main text, but for both methods, M1 and M4, separately.

3. Supporting Results

3.1 Root and stone contents in the soil samples

This section describes stones ≥ 0.01 m wide roots >0.0005 m diameter in the soil samples. Note that smaller items were ground up along with the rest of the soil, which was possible as the stones were mostly soft mudstone plus only a few quartz specs. Only two stones were extracted: volume= 33,500 mm^3 and 19,600 mm^3, C wt%= 0.17 and 0.78 respectively. In 90 soil samples, 22 contained roots: volume min=0.016 mm^3, max=29,500 mm^3 (a piece of coarse root), mean=2,300 mm^3, median=466 mm^3.

3.2 Alternative equations for bulk density as a function of C wt%

Supporting Table S1. Examples of equations for bulk density as a function of C wt% (y=*f*(x)). The solutions each have similar matches for our data though with slightly different curvatures. The different formulation types may be best suited to different soil types. Caveat: the ln term is not suitable for very small values of C wt%, because it approaches infinity. (Probability for each solution) *P*<0.005.

y=*f*(x)	df	adjR^2	a (SD) P(t) (kg m^{-3})	b (SD) P(t) (kg m^{-3})	c (SD) P(t) (kg m^{-3})	y intercept (kg m^{-3})
$a + b\sqrt{\mathrm{x}} - c\sqrt{\sqrt{\mathrm{x}}}$	88	0.77	3,455(320) <0.001	448.1(110) <0.001	2,397(400) <0.001	3,500
$a + b\mathrm{x} - c\sqrt{\sqrt{\mathrm{x}}}$	88	0.77	2,914(220) <0.001	22.78(6.1) <0.001	1,428(190) <0.001	2,900
$a + b/(c + \mathrm{x})$	88	0.77	184.1(55) <0.005	4,257(860) <0.001	2.089(0.53) <0.001	2,200
$a + bx - c\sqrt{x}$	88	0.79	2136(116) <0.001	53.89(10) <0.001	645.4(85) <0.001	2,100
$a + b\sqrt{\mathrm{x}} - c\log_e \mathrm{x}$	87	0.78	1,408(65) <0.001	72.96(46) <0.2	431.4(71) <0.001	-
$a + b\mathrm{x}^2 - c\log_e \mathrm{x}$	87	0.77	1,485(540)	7.829(0.059) <0.2	367.7(38)	-

3.3 Soil carbon density and cumulative SOC

The SOC densities for the M1 and differentiated-M4 differed only by a maximum of 7% down the profile (Supporting Fig. 1). The effect on M4 of fixing SOC density at 0 m to the lignomor average (C0) was negligible because it only had a localised effect, not multiplicative down the profile, as would have been the case with M1. For both under-trunk and under-humus soil, M4 was chosen as most representative for cumulative SOC (Supporting Table S2). M4 was considered more reliable than M1 due to the higher likelihood of bias during regression for M1.

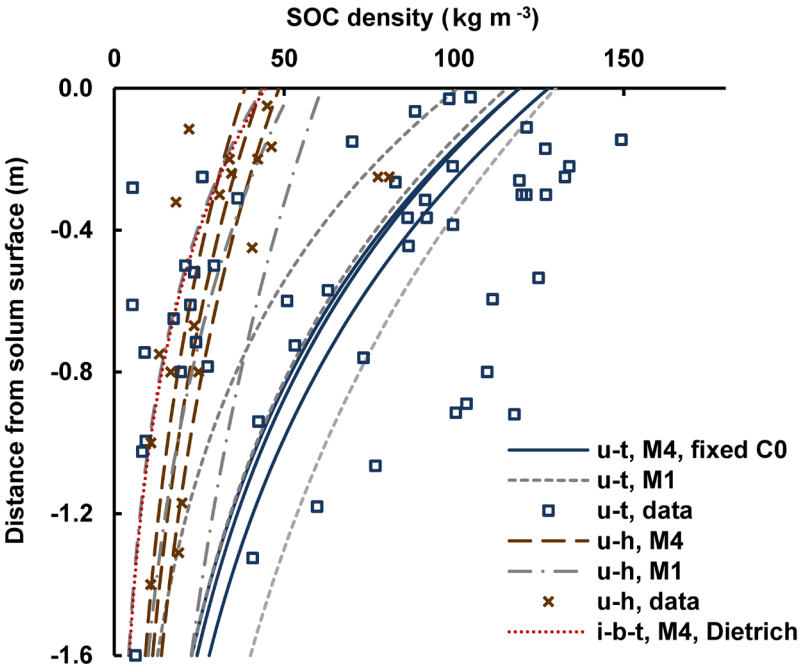

Supporting Fig. 1 SOC density location comparisons, for M1 and M4. The equations for the regression curves for M1 and M4 are 'Supporting Equation 1' and 'Eq2' (from the main text), respectively. 'u-t'= under- trunk, 'u-h'= under-humus area, 'i-b-t'= in-between-trees. Each regression curve for u-t and u-h, is a triplet, with the two outer curves being 1 standard deviation of regression parameters.

Supporting Table S2

Cumulative SOC, and depth at 90% of total. Numbers in brackets are 95% confidence intervals.

Method	Restraint	Cumulative SOC (Mg ha^{-1})	Depth at 90% of total (m)
		under-trunk	
M1	none	1138 (781–1768)	-2.27
M4	C0 at 0 m	1202 (1137–1277)	-2.32
M4	none	1223 (1152–1306)	-2.44
		under-humus	
M1	none	505 (300–986)	-2.22
M4	none	516 (473–572)	-2.73
		in-between-trees, derived from Dietrich (2012)	
M1	none	264 (144–605)	-1.26
M4	none	309 (295–324)	-1.59

For both M1 and M4, within the tree footprint, 90% of the SOC was calculated to be within ~2.6 m of the solum surface (Supporting Table S3, Supporting Fig. S2). The cumulative SOC down to only 0.3 m under-humus was: M1 135 (81-263) Mg ha^{-1} and M4 115 (106-128) Mg ha^{-1}.

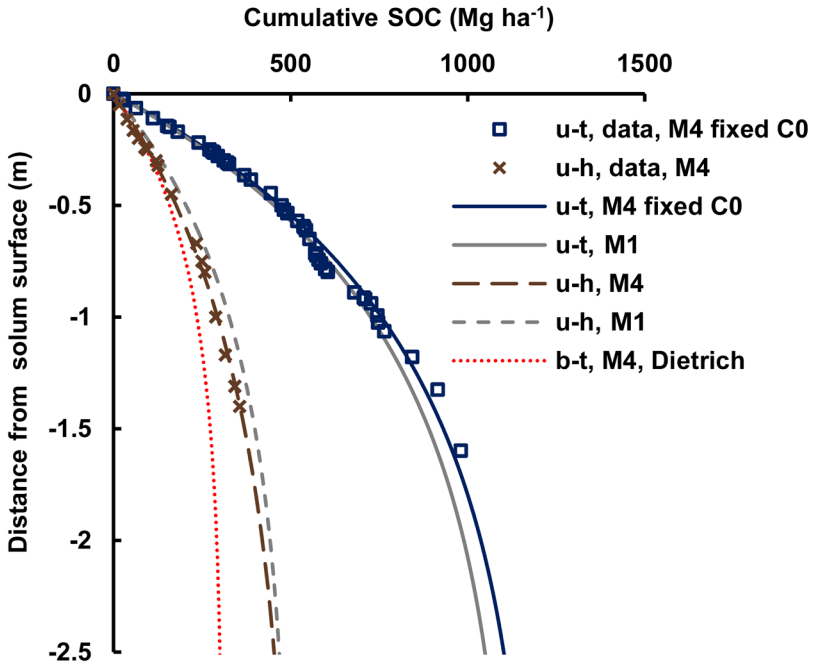

Supporting Fig. S2 Cumulative SOC, data and regression equations for different regions with respect to tree location: u-t= under-trunk, u-h= under-humus-area, b-t= in-between-trees. The equations for the regression curves for M1 and M4 are 'Supporting Equation 2' and 'Eq1' (from the main text), respectively.

3.4 Stand-level carbon

The overall effect of including near-tree SOC in mixed-forests, the 'Extra-SOC', was 7(3–12)% and 8(5–12)% more SOC, for methods M4 and M1 respectively, than is usually reported for such forests (Supporting Table S3).

Supporting Table S3

Stand-level effect on cumulative SOC (to 90% of total) from 'Extra-SOC', compared with in-between-trees (Dietrich, 2012). Numbers in brackets are 95.4% confidence intervals.

Method	In-between-trees (Mg ha^{-1}), derived from Dietrich (2012)	New total SOC (Mg ha^{-1})	Extra-SOC (%)
		All 10 plots	
M1	264	284	7.9(4.7–12)
M4	309	330	6.9(3.2–12)
		Seven *E. regnans*-dominated plots	
M1	264	287	8.9(5.4–14)
M4	309	332	7.6(3.6–13)
		Two most C-dense plots	
M1	264	296	12.4(7.4–20)
M4	309	341	10.6(5.0–18)

4. Supporting Discussion

Why does M4 indicates a higher cumulative SOC than integrated-M1, (e.g. 1223 compared with 1145 for under-trunk (7% higher), and 515 compared with 506 for under-humus (2% higher)) (Supporting Fig. 2)? The alternative question is: does M1 underestimate the cumulative SOC? One possibility is that M1 was more reliant on nonlinear regression for derivation of the equation parameters and there were fewer data points deeper down, which could bias its derivation. Note however that this effect does not transcribe to the Extra-SOC, which is higher for M1 than for M4, because that is a comparison between zones in the forest, rather than between calculation methods.

Supporting Table S4.
List of example tree species that may have substantial amounts of lignomor under the trunks of mature individuals. This is not an exhaustive list of likely species. Species were selected from their potential trunk diameter, DBH ≥ 1.5 m, combined with potential longevity ≥ 250 years. The individual DBHs and longevities cited may not be from the largest or oldest individuals (respectively). There are two main caveats: (a) it is in the absence of intense fire to-date for the tree, and (b) the lignomor's half-life of course determines for how long it remains *in situ*, which may depend on the tree species, fungal/bacteria species (that decomposed the roots), microclimate and soil etc. The DBHs and longevities are suffixed with a citation number, which links to a reference at the bottom of the table. Citation number '7' includes the internet moniker of the provider of the data to that online database.

Species name (ideal forest type)	Common name(s)	DBH max (m)	Longevity max (years)
Adansonia digitata	baobab	8.91 [7/joosto]	~2,000 [7/Tilazt]
Afzelia xylocarpa	makha tree	2.00 [48]	>200 [47]
Agathis australis	kauri pine	5.14 [24]	>1,200 [19]
Agathis microstachya	bull kauri	2.13 [33]	1060 [33]
Albizia saman	rain tree/ monkey pod	2.50 [8]	~500 [35]
Annamocarya sinensis	Chinese hickory	1.50 [43]	>250 [43]
Apeiba membranacea	monkey comb	1.53 [34]	338 [34]
Atherosperma moschatum	sassafras	2.00 [36]	250 [23]
Bertholletia excels	Brazil nut	2.10 [46]	~400 [45]
Calocedrus macrolepsis	bách xan/ Chinese incense cedar	2.00 [44]	>300 [43]
Carapa guianensis	andiroba	1.57 [34]	442 [34]
Cariniana micrantha	castanha de macaco/ tauarí	2.75 [39]	~450 [39]
Carpinus betulus	hornbeam	2.18 [7/Owen Johnson]	~460 [7/Aedificius]
Castanea sativa	sweet chestnut	7.14 [7/Giant Trees Foun.]	~3,000 [7/Giant Trees Foun.]
Ceiba pentandra	kapok	3.00 [30]	500 [14]
Cinnamomum camphora	camphor tree	7.08 [7]	~1920 [7/Weber]
Corymbia calophylla	marri	3.98 [2]	>450 [32]
Cryptomeria japonica	Liu shan/ Japanese cedar/ sugi	3.50 [7/Jenny]	~2,000 [7/Jenny]
Dipterocarpus alatus	apitong / yang naa	5.00 [11]	≥300 [12]
Eucalyptus cypellocarpa	mountain grey gum	2.50 [51]	295 [52]
Eucalyptus delegatensis (mixed-forest)	gum-top-stringybark/ alpine ash/ white- top	5.73 [2]	380 [38]
Eucalyptus diversicolor	karri	4.14 [2]	350 [41]
Eucalyptus fastigata	brown barrell	3.50 [5]	~250 [42]
Eucalyptus marginata	jarrah	3.28 [2]	>450 [32]
Eucalyptus obliqua (mixed-forest)	stringy bark/ messmate	6.53 [2]	350 [37]

Eucalyptus pilularis	blackbutt	4.81 [2]	400 [2]
Eucalyptus regnans (mixed-forest)	swamp gum/ mountain ash	10.78 [4]	520 [31]
Eucalyptus viminalis	manna gum	3.50 [2]	~400 [40]
Fagus sylvatica	lowland beech	1.72 [10]	~520 [7/Sacro Sciuto]
Ficus macrophylla	Moreton Bay fig	9.23 [2]	270 [13]
Hopea odorata	ta-khian/ thingan	1.70 [48]	~380 [47]
Lagorostrobus franklinii	Huon pine	1.83 [50]	2,200 [49]
Nothofagus cunninghamii	myrtle beech	3.54 [2]	500 [23]
Nyssa aquatica	water tupelo/ tupelo gum	3.83 [27]	~275 [7/Scott Wade]
Petersianthus quadrialatus	Philipine rosewood/ toog tree	3.60 [7]	~265 [7/DBZT]
Pinus longaeval	bristlecone pine	4.71 [7/Giant Trees Foun.]	~5,000 [7]
Pinus sylvestris (wet temperate forest)	Scotts pine	1.90 [7/Butler & Green]	589 [7/George]
Platanus orientalis	*oriental plane-tree*	8.59 [7/ 'George']	~2070 [7/Turgut68]
Pseudotsuga menziesii	Douglas fir	7.62 [24]	~1,020 [7/KoutaR]
Pterocarpus officinalis	bloodwood/ dragon blood tree	2.25 [34]	208 [34]
Quercus alba	white oak	2.68 [27]	464 [22]
Quercus chrysolepis	canyon live oak	4.03 [27]	464 [22]
Querus robur	pedunculate oak	4.81 [7/Windemuller]	600 [16]
Quercus petraea	sessile oak	4.46 [7/Ancient Tree Hunt]	~1018 [7/ van Boeschoten]
Sequoia semipervirens	redwood	6.37 [19]	2,000 [25]
Sequoia giganteum	giant sequoia	8.47 [19]	~3,200 [7/Sillet]
Taxodium distichum	bald-cypress	5.34 [27]	~2,070 [7/arkansastreehugger]
Taxodium mucronatum	Montezuma cypress	12.22 [24]	~1,420 [7/Conifers]
Taxus baccata	European yew	5.43 [18]	~1,500 [18]
Tetrameles nudiflora	kajoolaboo/ binong/ shidam	7.70 [7/Meyer]	>200 [53]
Tsuga canadensis	Eastern hemlock	1.75 [21]	450 [20]

References for Table S4: [1] Maiden (1904); [2] McIntosh (2018); [3] Maiden (1917); [4] Ashton (1975); [5] Taylor (1993); [6] PFAF (2020); [7] MonumentalTrees.com (2020) ; [8] Hensleigh and Holaway (1988); [9] Vandekerkhove et al. (2018); [10] Straußberger (2003); [11] Smitinand et al. (1980); [12] Dyrmose et al. (2017); [13] Ipswich Council (2018); [14] Cristóbal (2000); [15] Heritage Council of Victoria (2004); [16] Rodgers (1941); [17] Classic History (2019); [18] Harte (1996); [19] Mace (1996); [20] Villeneuve and Brisson (2003); [21] Blozan (2006); [22] Pederson (2010); [23] Gilbert (1959); [24] Newcastle Morning Herald (1937); [25] Williams and Sillett (2007); [26] Ruting (2015); [27] American Forests (2014); [28] Homewood (2019); [29] Jensen (1999); [30] Slik (2009); [31] Wood et al. (2010); [32] Whitford (2014); [33] Ogden (1981); [34] Lieberman et al. (1985); [35] Ajaytao Photography (2020); [36] Read and Hill (1988); [37] Koch et al. (2008); [38] Bowman and Kirkpatrick (1984); [39] Worbes and Junk (1999); [40] Hickey et al. (2000); [41] Rayner (1992); [42]

Banks (1990); [43] Zuidema et al. (2011); [44] ALA (2020); [45] Jochen Schongart (2015); 46 Brienen and Zuidema (2006); [47] Baker et al. (2005); [48] Bunyavejchewin et al. (2001); [49] Ogden (1978); [50] Sharland (1940); [51] Lindenmayer et al. (1993); [52] Ambrose (1982); [53] Kerkar (2018)

Supporting References

Ajaytao Photography, 2020. Albizia saman – Rain tree – Ajaytao. Available at: https://ajaytaobotanicalblog.wordpress.com/tag/samanea-saman/, [accessed 04-May-2020].

ALA, 2020. *Calocedrus macrolepis* Kurz. Available at: https://bie.ala.org.au/species/NZOR-6-4065, [accessed 04-May-2020].

Ambrose, G.J., 1982. An ecological and behavioural study of vertebrates using hollows in eucalypt branches, La Trobe University, Melbourne, Australia, 447 pp.

American Forests, 2014. Spring 2014 National Register Of Big Trees, American Forests. Available at: https://www.americanforests.org/wp-content/uploads/2014/06/Spring-2014-Register-PDF-web.pdf, [accessed 05-April-2020].

Ashton, D.H., 1975. The root and shoot development of *Eucalyptus regnans* F. Muell. Australian Journal of Botany, 23, 867-887, doi:10.1071/BT9750867.

Ashton, D.H., 1981. Fire in tall open-forests (wet sclerophyll forests). In: A.M. Gill, R.H. Groves and I.R. Noble (Editors), Fire and the Australian Biota. Australian Academy of Science, Canberra, pp. 339-366.

Baker, P.J., Bunyavejchewin, S., Oliver, C.D. and Ashton, P.S., 2005. Disturbance history and historical stand dynamics of a seasonal tropical forest in western Thailand. Ecological Monographs, 75, 317–343.

Banks, J.C.G., 1990. The fire histories of two forest types in Glenborg State Forest, NSW. A report to the joint scientific committee on the south-east forests., Department of Forestry, Australian National University, Canberra, Australia. Available at: [accessed.

Blozan, W., 2006. Laurel Branch Leviathan climb, The Native Tree Society. Available at: http://www.nativetreesociety.org/tsuga/laurel_branch/laurel_branch_leviathan_climb.htm, [accessed 27-April-2020].

Bowman, D.M.J.S. and Kirkpatrick, J.B., 1984. Geographic variation in the demographic structure of stands of *Eucalyptus delegatensis* R. T. Baker on dolerite in Tasmania. Journal of Biogeography, 11, 427-437.

Brienen, R.J.W. and Zuidema, P.A., 2006. Lifetime growth patterns and ages of Bolivian rain forest trees obtained by tree ring analysis. Journal of Ecology, 94, 481-493.

Bunyavejchewin, S., Baker, P.J., LaFrankie, J.V. and Ashton, P.S., 2001. Stand structure of a seasonal dry evergreen forest at Huai Kha Khaeng Wildlife Sanctuary, western Thailand. Natural History Bulletin Of The Siam Society, 49, 89-106.

Classic History, 2019. The American Chestnut Tree, www.classichistory.net. Available at: http://www.classichistory.net/archives/chestnut-trees, [accessed: 26-April-2020].

Cremer, K.W., 1962. The Effect of Fire on Eucalypts Reserved for Seeding. Australian Forestry, 26, 129-154, doi:10.1080/00049158.1962.10675921.

Cristóbal, C.M.D.n., 2000. Panorama Histórico Forestal de Puerto Rico Universidad De Puerto Rico, San Juan, Puerto Rico, 680 pp.

Dean, C. and Horn, E., 2019. A hard, high-carbon, lignomor with conchoidal fracture: cunnite, from mature myrtle beech (*Nothofaus cunninghamii* (Hook. f.) Oerst.). Geoderma, In Press, doi:10.1016/j.geoderma.2018.07.006.

Dietrich, P., 2012. Carbon stocks in coarse woody debris and soil in the mixed forests and the rainforests in southern Tasmania. MSc Thesis, Technische Universität, Dresden, Germany.

Dyrmose, A.-M.H., Turreira Garcia, N., Theilade, I. and Meilby, H., 2017. Economic importance of oleoresin (Dipterocarpus alatus) to forest-adjacent households in Cambodia. Siam Society. Natural History Bulletin, 62, 67-84.

Gilbert, J.M., 1959. Forest succession in the Florentine Valley, Tasmania. papers and Proceedings of the Royal Society of Tasmania, 93, 129-151.

Grove, S.J., Stamm, L. and Wardlaw, T.J., 2011. How well does a log decay-class system capture the ecology of decomposition? – A case-study from Tasmanian Eucalyptus obliqua forest. Forest Ecology and Management, 262, 692-700, doi:10.1016/j.foreco.2011.05.005.

Harte, J., 1996. How old is that yew? At the Edge, 4, 1-7.

Hensleigh, T.E. and Holaway, B.K., 1988. Agroforestry species for the Philippines. US Peace Corps Technology Support Center, Manilla, Philippines, 404 pp.

Heritage Council of Victoria, 2004. Nothofagus cunninghamii, Heritage Council of Victoria,. Available at: https://vhd.heritagecouncil.vic.gov.au/places/70761, [accessed 26-04-2020].

Hickey, J.E., Kostoglou, P. and Sargison, G.J., 2000. Tasmania's tallest trees. Tasforests, 12, 105-122.

Homewood, 2019. Maribyrnong City Council Significant Tree Register 2019 Draft For Consultation Maribyrnong City Council. Available at: file:///F:/cdean/doco/papers/adjust_SOC/Goederma/other_papers/Draft-Maribyrnong-Significant-Tree-Register-2019_addedums-19-27-Feb.pdf, [accessed 04-May-2020].

Ipswich Council, 2018. 270-year-old Moreton Bay Fig Tree part of Ipswich's heritage character. Available at: https://www.ipswich.qld.gov.au/about_council/media/articles/2018/270-year-old-moreton-bay-fig-tree-part-of-ipswichs-heritage-character, [accessed: 26-04-2020].

Jensen, M., 1999. Trees Commonly Cultivated In Southeast Asia. An Illustrated Field Guide. Food and Agriculture Organization of the United Nations, Bangkok, Thailand.

Jobággy, G.J. and Jackson, R.B., 2002. The vertical distribution of soil organic carbon and its relation to climate and vegetation. Ecological Applications, 10, 423-436, doi:10.2307/2641104.

Jochen Schongart, R.G., Sinomar Ferreira da Fonseca-Junior, Torbjørn Haugaasen, 2015. Age and growth patterns of brazil nut trees (*Bertholletia excelsa* Bonpl.) in Amazonia, Brazil. Biotropica, 47, 550-558.

Jurgensen, M.F. et al., 1997. Impacts of timber harvesting on soil organic matter, nitrogen, productivity, and health of inland Northwest forests. Forest Science, 43, 234-251.

Kempen, B., Brus, D.J. and Stoorvogel, J.J., 2011. Three-dimensional mapping of soil organic matter content using soil type–specific depth functions. Geoderma, 162, 107-123, doi:10.1016/j.geoderma.2011.01.010.

Kerkar, R.P., 2018. A green giant that has stood the test of time. Times of India.

Kirkpatrick, J.B., Peacock, R.J., Cullen, P.J. and Neyland, M.G., 1988. The Wet Eucalypt Forests of Tasmania. Tasmanian Conservation Trust Hobart, Hobart.

Koch, A.J., Driscoll, D.A. and Kirkpatrick, J.B., 2008. Estimating the accuracy of tree ageing methods in mature *Eucalyptus obliqua* forest, Tasmania. Australian Forestry, 71, 147–159.

Lieberman, D., Lieberman, M., Hartshorn, G. and Peralta, R., 1985. Growth rates and age-size relationships of tropical wet forest trees in Costa Rica. Journal of Tropical Ecology, 1, 97-109.

Lindenmayer, D.B., Cunningham, R.B., Donnelly, C.F., Tanton, M.T. and Nix, H.A., 1993. The abundance and development of cavities in *Eucalyptus* trees: a case study in the montane forests of Victoria, southeastern Australia. Forest Ecology and Management, 60, 77-104.

Mace, B., 1996. Mueller— Champion of Victoria's giant trees. Victorian Naturalist, 113, 198-207.

Maiden, J.H., 1904. Where are the Largest Trees in the World, The Sydney Morning Herald, Sydney, pp. 3.

Maiden, J.H., 1917. Forestry Handbook. Part Il. Some of the Principal Commercial Trees of New South Wales. Forest Department of New South Wales, Sydney, 224 pp.

Maser, C., Aderson, R.G. and Cromack, K., Jr. [and others], 1979. Dead and down woody material. In: J.W. Thomas (Editor), Wildlife habitats in managed forests: the Blue Mountains of Oregon and Washington. U.S. Department of Agriculture In cooperation with: Wildlife Management Institute and the U.S. Department of the Interior, Bureau of Land Management, Washington, DC, pp. 78-95.

McFee, W.W. and Stone, E.L., 1966. The persistence of decaying wood in the humus layers of northern forests. Soil Science of America Proceedings, 30, 513-516, doi:10.2136/sssaj1966.03615995003000040032x.

McIntosh, D., 2018. National Register of Big Trees. Australia's Champion Trees. Available at: http://www.nationalregisterofbigtrees.com.au/, [accessed 26-April-2020].

Mishra, U. et al., 2009. Predicting Soil Organic Carbon Stock Using Profile Depth Distribution Functions and Ordinary Kriging. Soil Science Society of America Journal, 73, 614, doi:10.2136/sssaj2007.0410.

MonumentalTrees.com, 2020. Monumental trees. Available at: https://www.monumentaltrees.com/en/, [accessed 25-April-2020].

Newcastle Morning Herald, 1937. Forest Giants. The World's Biggest Trees, Newscastle Morning Herald and Miners' Advocate, Newcastle, NSW.

Ogawa, H., Yoda, K. and Kira, T., 1961. A preliminary survey on the vegetation of Thailand, Nature and Life in Southeast Asia. Fauna and Flora Research Society, Kyoto, Japan, pp. 20–158.

Ogden, J., 1978. On the dendrochronological potential of Australian trees. Australian Journal of Ecology, 3, 339-356.

Ogden, J., 1981. Dendrochronological studies and the determination of tree ages in the Australian tropics. Journal of Biogeography, 8, 405-420.

Pederson, N., 2010. External characteristics of old trees in the Eastern deciduous forest. Natural Areas Journal, 30, 396-407.

PFAF, 2020. Plants For a Future online database, Plants For a Future. Available at: https://pfaf.org/user/Plant.aspx?LatinName=Dysoxylum+fraserianum, [accessed 04-May-2020].

Polglase, P.J., Adams, M.A. and Attiwill, P.M., 1994. Measurement and Modelling of Carbon Storage in a Chronosequence of Mountain Ash Forests: Implications for Regional and Global Carbon Budgets. State Electricity Commission, Melbourne, Victoria, Australia, 62 pp.

Ratkowsky, A.D., 1990. Handbook of Nonlinear Regression Models. Marcel Dekker, New York.

Rayment, G.E. and Lyons, D.J., 2011. Carbonates by pressure change-transducer (method 19B2), Soil Chemical Methods-Australasia. CSIRO, Collingwood, VIC, Australia, pp. 420-422.

Rayner, M.E., 1992. Application of dendrochronology, stem analysis and inventory data in the estimation of tree and stand ages in karri forest. Technical Report 0816-6757 ; No. 27. Department of Conservation and Land Management, Perth, Western Australia, 19 pp.

Read, J. and Hill, R.S., 1988. The dynamics of some rainforest associations in Tasmania. Journal of Ecology, 76.

Rodgers, J., 1941. The English Woodland. Batsford, London, 132 pp.

Roxburgh, S.H. et al., 2006. Organic carbon partitioning in soil and litter in subtropical woodlands and open forests: a case study from the Brigalow Belt, Queensland. The Rangeland Journal, 28, 115-125, doi:10.1071/rj05015.

Ruting, N., 2015. Heritage Trees in the Domain, Royal Botanic Garden Sydney. Available at: http://www.landarc.com.au/uploads/8/2/3/0/8230432/rbg_domain_heritage_trees_noel_ruting.pdf, [accessed 04-May-2020].

Salmi, T., Määttä, A., Anttila, P., Ruoho-Airola, T. and Amnell, T., 2002. Detecting Trends of Annual Values of Atmospheric Pollutants By The Mann-Kendall Test and Sen's Slope Estimates -The Excel Template Application MAKESENS, Publications on Air Quality, No. 31. Finnish Meteorological Institute, Helsinki, pp. 36.

Schmidt, M. and Lipson, H., 2009. Distilling free-form natural laws from experimental data. Science, 324, 81-5, doi:10.1126/science.1165893.

Sharland, M.S.R., 1940. Huon pine. Tasmania's disappearing softwood. Walkabout, 6, 35-38.

Sherrod, L.A., Dunn, G., Peterson, G.A. and Kolberg, R.L., 2002. Inorganic carbon analysis by modified pressure-calcimeter method. Soil Science Society of America Journal, 66, 299-305, doi:10.2136/sssaj2002.2990.

Slik, J.W.F., 2009. Pants of Southeast Asia. Available at: http://www.asianplant.net/, [accessed 04-May-2020].

Smitinand, T., Phengklai, C. and Santisuk, T., 1980. The manual of Dipterocarpaceae of mainland South-east Asia. Forest Herbarium, Bangkok, Thailand, 133 pp.

Straußberger, R., 2003. Buchen-Naturwaldreservate - Perlen im Oberpfälzer Wald. LWFWissen, 43, 47-77.

Strukelj, M. et al., 2013. Chemical transformations in downed logs and snags of mixed boreal species during decomposition. Canadian Journal of Forest Research, 43, 785-798, doi:10.1139/cjfr-2013-0086.

Taylor, M., 1993. Anger at decision to lift ban on logging, The Canberra Times, Canberra, Australia, pp. 18.

Turner, P.A.M., Balmer, J. and Kirkpatrick, J.B., 2009. Stand-replacing wildfires? The incidence of multicohort and single-cohort Eucalyptus regnans and E. obliqua forests in southern Tasmania. Forest Ecology and Management, 258, 366-375, doi:10.1016/j.foreco.2009.04.021.

Vandekerkhove, K. et al., 2018. Very large trees in a lowland old-growth beech (Fagus sylvatica L.) forest: Density, size, growth and spatial patterns in comparison to reference sites in Europe. Forest Ecology and Management, 417, 1-17, doi:10.1016/j.foreco.2018.02.033.

Villeneuve, N. and Brisson, J., 2003. Old-growth forests in the temperate deciduous zone of Quebec: Identification and evaluation for conservation and research purposes. The Forestry Chronicle, 79, 559-569.

Waksman, S.A., 1936. Humus. Origin, Chemical Composition and Importance in Nature. The Williams & Wilkins Company, Baltimore, USA, 511 pp.

Whitford, K., 2014. The age of jarrah (*Eucalyptus marginata*) and marri (*Corymbia calophylla*) trees, Department of parks and Wildlife, teh Government of Western Australia, Perth, Western Australia. Available at: https://library.dbca.wa.gov.au/static/Journals/080525/080525-81.pdf, [accessed 04-May-2020].

Williams, C.B. and Sillett, S.C., 2007. Epiphyte communities on redwood (Sequoia sempervirens) in northwestern California. The Bryologist, 110, 420–452.

Wood, S.W., Hua, Q., Allen, K.J. and Bowman, D.J.M.S., 2010. Age and growth of a fire prone Tasmanian temperate old-growth forest stand dominated by *Eucalyptus regnans*, the world's tallest angiosperm. Forest Ecology and Management, 260, 438-447, doi:10.1016/j.foreco.2010.04.037.

Worbes, M. and Junk, W.J., 1999. How old are tropical trees? The persistence of a myth. IAWA Journal, 20, 255-260.

Zuidema, P.A., Vlam, M. and Chien, P.D., 2011. Ages and long-term growth patterns of four threatened Vietnamese tree species. Trees, 25, 29-38, doi:10.1007/s00468-010-0473-2.